Virology 563 (2021) 1–19

Contents lists available at ScienceDirect

Virology

journal homepage: www.elsevier.com/locate/virology

Targeting conserved co-opted host factors to block virus replication: Using allosteric inhibitors of the cytosolic Hsp70s to interfere with tomato bushy stunt virus replication

Melissa Molho [1], K. Reddisiva Prasanth [1], Judit Pogany, Peter D. Nagy [*]

Department of Plant Pathology, University of Kentucky, Lexington, KY, 40546, USA

ARTICLE INFO

Keywords:
Tomato bushy stunt virus
Carnation Italian ringspot virus
hsp70
Allosterick inhibitors
Virus replication
Antiviral
Yeast
Plant
Replicase

ABSTRACT:

To further our understanding of the pro-viral roles of the host cytosolic heat shock protein 70 (Hsp70) family, we chose the conserved *Arabidopsis thaliana* Hsp70-2 and the unique Erd2 (early response to dehydration 2), which contain Hsp70 domains. Based on *in vitro* studies with purified components, we show that AtHsp70-2 and AtErd2 perform pro-viral functions equivalent to that of the yeast Ssa1 Hsp70. These functions include activation of the tombusvirus RdRp, and stimulation of replicase assembly. Yeast-based complementation studies demonstrate that AtHsp70-2 or AtErd2 are present in the purified tombusvirus replicase. RNA silencing and over-expression studies in *Nicotiana benthamiana* suggest that both Hsp70-2 and Erd2 are co-opted by tomato bushy stunt virus (TBSV). Moreover, we used allosteric inhibitors of Hsp70s to inhibit replication of TBSV and related plant viruses in plants. Altogether, interfering with the functions of the co-opted Hsp70s could be an effective antiviral approach against tombusviruses in plants.

1. Introduction

Positive stand (+)RNA viruses have small genomes and their replication depends on many co-opted host factors. Major efforts with several animal viruses using genomic and proteomic approaches have led to the identification of hundreds of pro-viral or antiviral host factors (Acosta et al., 2014; de Wilde et al., 2018; Diamond and Schoggins, 2013; Krishnan et al., 2008; Li et al., 2009a; Neufeldt et al., 2018; Yasunaga et al., 2014). Interestingly, systematic genome-wide screens have also been performed with yeast (*Saccharomyces cerevisiae*), which can support the replication of plant tomato bushy stunt virus (TBSV) and the unrelated brome mosaic virus and the insect Flock house virus and Nodamura virus (Gancarz et al., 2011; Jiang et al., 2006; Kushner et al., 2003; Nagy, 2016; Nagy, 2017; Panavas et al., 2005b; Pogany et al., 2010; Serviene et al., 2005; Shah Nawaz-Ul-Rehman et al., 2013). Although a large number of host factors is specific for different viruses, the emerging theme from the large-scale studies and from follow-up studies with a number of subverted proteins is that co-opted host factors bear many functional resemblances (Huang et al., 2012; Nagy, 2016, 2017; Nagy and Pogany, 2012; Sanfacon, 2017; Shulla and Randall, 2012; Wang, 2015; Zhang et al., 2019). For example, subverted host factors facilitate the assembly of the membrane-bound viral replicase complexes (VRCs), which consist of viral- and host-coded proteins and the viral RNA templates, and the biogenesis of large viral replication organelles (VROs) harboring clusters of VRCs (Altan-Bonnet, 2017; de Castro et al., 2013; de Wilde et al., 2018; Fernandez de Castro et al., 2017; Hyodo and Okuno, 2020; Nagy, 2016; Nagy and Pogany, 2012; Neufeldt et al., 2018).

Among the most wide-spread host factors involved in (+)RNA virus infections are the heat shock proteins (Hsps) (Nagy, 2020; Nagy et al., 2011; Taguwa et al., 2015). The best-studied heat shock proteins in viral replication are the Hsp70 and Hsp90 families of conserved Hsp proteins that have molecular chaperone functions (Clerico et al., 2015; Duncan et al., 2015; Moran Luengo, Mayer, and Rudiger, 2019; Rosenzweig et al., 2019). Hsp70s are involved in maintenance of protein homeostasis, protein folding and preventing protein aggregation, refolding of denatured proteins, protein degradation, autophagy and transport of proteins through cellular membranes. Hsp70s bind to surface-exposed hydrophobic amino acid stretches and refold the client proteins in an ATP-dependent manner. Successive binding and release of the substrate proteins by Hsp70s usually depends on Hsp40 co-chaperones. Several members of Hsp70s are expressed constitutively in cells (called Hsc70s),

* Corresponding author.
E-mail address: pdnagy2@uky.edu (P.D. Nagy).
[1] These authors contributed equally.

https://doi.org/10.1016/j.virol.2021.08.002
Received 31 March 2021; Received in revised form 3 August 2021; Accepted 4 August 2021
Available online 6 August 2021

whereas other members are transiently expressed in response to various stresses, such as heat, cold, drought, oxidative stresses or pathogen infections (Cazale et al., 2009; Ferradini et al., 2015; Moran Luengo, Mayer, and Rudiger, 2019; Rosenzweig et al., 2019; Wang et al., 2004). Hsp70s are localized not only in the cytosol, but in all organelles and localization to distinct subcellular compartments implies functional specificity for different members. The *Arabidopsis* genome encodes 18 different members of Hsp70s, including 14 in the DnaK/Ssa subfamily and 4 in the Hsp110/Sse subfamily (Lin et al., 2001). Five Hsp70s (Hsp70-1-to-5) are cytosolic, similar to the Ssa subfamily in yeast. There are no obvious yeast Ssb-like Hsp70s in the *Arabidopsis* genome (Lin et al., 2001).

TBSV is a small (+)RNA virus that has been intensively used to study virus replication, recombination, and virus - host interactions based on yeast (*Saccharomyces cerevisiae*) model host (Nagy and Pogany, 2012; Nagy et al., 2014; Panavas and Nagy, 2003). TBSV expresses only two replication proteins, including p33 RNA chaperone and the $p92^{pol}$ RdRp (RNA-dependent RNA polymerase) protein. The tombusvirus p33 protein recruits the TBSV (+)RNA to the cytosolic surface of peroxisomal membranes for replication (Nagy et al., 2012; Panavas et al., 2005a; Pogany et al., 2005; Stork et al., 2011). The assembly of the functional VRC requires interaction between the viral p33 and $p92^{pol}$ RdRp protein (Panavas et al., 2005a; Panaviene et al., 2005; Pogany and Nagy, 2008, 2012). Importantly, the assembly and functions of VRCs are greatly affected by host components, such as Ssa1/2 (Hsp70), the eukaryotic elongation factor 1A (eEF1A), eEF1Bγ, ESCRT (endosomal sorting complexes required for transport) proteins, DEAD-box RNA helicases, Ubc2/Rad6/Cdc34 ubiquitin-conjugating enzymes and glycolytic/fermentation enzymes and lipids, such as sterols, phospholipids and phosphoinositides (Feng et al., 2019; Huang and Nagy, 2011; Imura et al., 2015; Kovalev et al., 2020; Li et al., 2008, 2009b, 2010; Pogany and Nagy, 2012; Sasvari et al., 2011, 2020; Sharma, Sasvari, and Nagy, 2010, 2011; Xu and Nagy, 2015a).

The molecular functions of co-opted Hsp70s have been studied in some details during TBSV replication, however, many of the experiments relied on the yeast Ssa1 and Ssa2 Hsp70s. For example, it has been shown that Hsp70 is recruited from the cytosol to the site of TBSV replication via its interaction with the p33 and $p92^{pol}$ replication proteins (Wang et al., 2009). Hsp70 is a permanent resident in the tombusvirus VRC (Serva and Nagy, 2006), and likely plays multiple roles during TBSV replication. Hsp70 affects the intracellular localization of the TBSV replication proteins, which are mislocalized to the cytosol in the absence of functional Hsp70s in yeast (Wang et al., 2009; Wang et al., 2009a,b). Hsp70 is also needed for viral p33 to bind to the cellular membrane *in vitro* (Wang et al., 2009). Moreover, Hsp70 affects the assembly of the tombusviral VRC (Pogany et al., 2008). Hsp70 is also required for the activation of the RdRp activity of $p92^{pol}$ protein *in vitro* (Pogany and Nagy, 2015). Additionally, Hsp70 is present in tombusvirus capsids, facilitating disassembly (Alam and Rochon, 2017). The yeast cell-free extract (CFE)-based and the purified replicase preparation-based *in vitro* studies with depleted Hsp70 demonstrated convincingly that Hsp70 is an essential host factor for TBSV replication (Pogany et al., 2008; Wang et al., 2009).

The emerging picture with plant viruses, including TBSV, is that many of the identified host factors hijacked by different plant viruses are common and conserved. This likely opens up the possibility to develop broad-range and durable antivirals targeting those common host factors. One of the outstanding candidates for such approaches is the cytosolic Hsp70 family, which is widely co-opted by an ever-increasing number of plant and animal viruses (Nagy et al., 2011; Taguwa et al., 2015). Therefore, we decided to further characterize the roles of the cytosolic Hsp70s in TBSV replication and to apply inhibitors of Hsp70s as antiviral approaches in this work.

To further extend our understanding of the roles of Hsp70s that might be involved in tombusvirus replication, in this paper we focused on the cytosolic *Arabidopsis* Hsp70s identified earlier in a yeast two-hybrid screen with p33 (Molho et al., 2021). These include Hsp70-1, Hsp70-2 and the unique Erd2 (early response to dehydration 2), which contain Hsp70-like domains (Kiyosue et al., 1994; Sung et al., 2001). *In vitro* studies with purified components revealed that both AtHsp70-2 and AtErd2 could activate the p92 RdRp, and stimulate the *in vitro* activity of the tombusvirus replicase. Finally, we applied allosteric inhibitors of Hsp70s to block TBSV replication *in vitro*, in yeast and plants. Altogether, it seems that interfering with the functions of the co-opted Hsp70s could be a strong antiviral approach in plants.

2. Results

The cytosolic *Arabidopsis* Hsp70 and AtErd2 proteins interact with the tombusvirus replication proteins. Our recently performed MYTH (membrane yeast two-hybrid) assay in yeast using an *Arabidopsis* cDNA library has identified the conserved *Arabidopsis* Hsp70-1, Hsp70-2 and the unique Erd2 proteins as interactors with the tombusvirus p33 replication protein in yeast (Molho et al., 2021). This suggests the involvement of several members of the Hsp70 family of molecular chaperones in TBSV replication in plants. Previous studies in yeast have shown that only the highly similar Ssa1 and Ssa2 (out of the 14 Hsp70 members in yeast) are co-opted by TBSV in yeast, suggesting that only the constitutively and highly-expressed cytosolic Hsp70s are co-factors for TBSV (Serva and Nagy, 2006; Wang et al., 2009; Wang et al., 2009a,b). However, there are only limited biochemical or genetic data whether the plant Hsp70s in general and in particular which Hsp70 member could specifically provide equivalent functions to the yeast Ssa1/2 during TBSV replication. Here we chose AtErd2 and AtHsp70-2, because AtHsp70-1 shows very high sequence identity with AtHsp70-2, suggesting functional overlaps.

To test if AtErd2 and AtHsp70-2 could facilitate TBSV replication similar to the yeast Ssa1/2, first we confirmed that the full-length AtErd2 and AtHsp70-2 interact with the p33 and p92 replication proteins in the MYTH assay (Fig. 1A). Then, we expressed the Flag-tagged AtErd2 and AtHsp70-2 in yeast, followed by affinity purification of 2xStrep-tagged p33 and p92 from the detergent-solubilized yeast membrane fraction, where the active VRCs are located (Serva and Nagy, 2006). These co-purification experiments clearly showed the robust co-purification of AtErd2 and AtHsp70-2 as seen for the yeast Ssa1 Hsp70 (Fig. 1B). These data suggest that AtErd2 and AtHsp70-2 are efficiently recruited into the tombusvirus replicase in yeast.

Erd2 and Hsp70–2 proteins are recruited into the tombusvirus replication compartment in *Nicotiana benthamiana*. To confirm that Erd2 and Hsp70-2 are recruited by tombusviruses into VROs in plant cells, we have conducted bimolecular fluorescence complementation (BiFC) experiments with TBSV p33 replication protein and AtErd2 and AtHsp70-2 in *N. benthamiana* leaves. The BiFC signals revealed specific interactions between AtErd2 and AtHsp70-2 and p33 replication proteins within the large VROs consisting of aggregated peroxisomes (Fig. 1C). Similar BiFC-based experiments with the closely-related carnation Italian ringspot virus (CIRV), whose VROs are built from aggregated mitochondria, also confirmed interaction between the CIRV p36 replication protein and AtErd2 and AtHsp70-2 within the VROs consisting of aggregated mitochondria (Fig. 1D).

Confocal microscopy analysis revealed that both AtErd2 and AtHsp70-2 are efficiently re-localized into the TBSV p33-BFP decorated VROs in *N. benthamiana* leaves infected with TBSV (Fig. 2A and B). We found that expression of the TBSV p33 replication protein alone (in the absence of viral replication) was enough to recruit either AtErd2 or AtHsp70-2 into the VRO-like compartments (Fig. 2A and B). Similar extensive re-localization of AtErd2 and AtHsp70-2 into VROs was observed when plants were infected with CIRV (Fig. 2C and D). The RFP-SKL (peroxisomal luminar marker protein) and RFP-Tim21 (mitochondrial marker protein) did not co-localize with AtErd2 and AtHsp70-2 when expressed in *N. benthamiana* in the absence of viral components (Fig. 2).

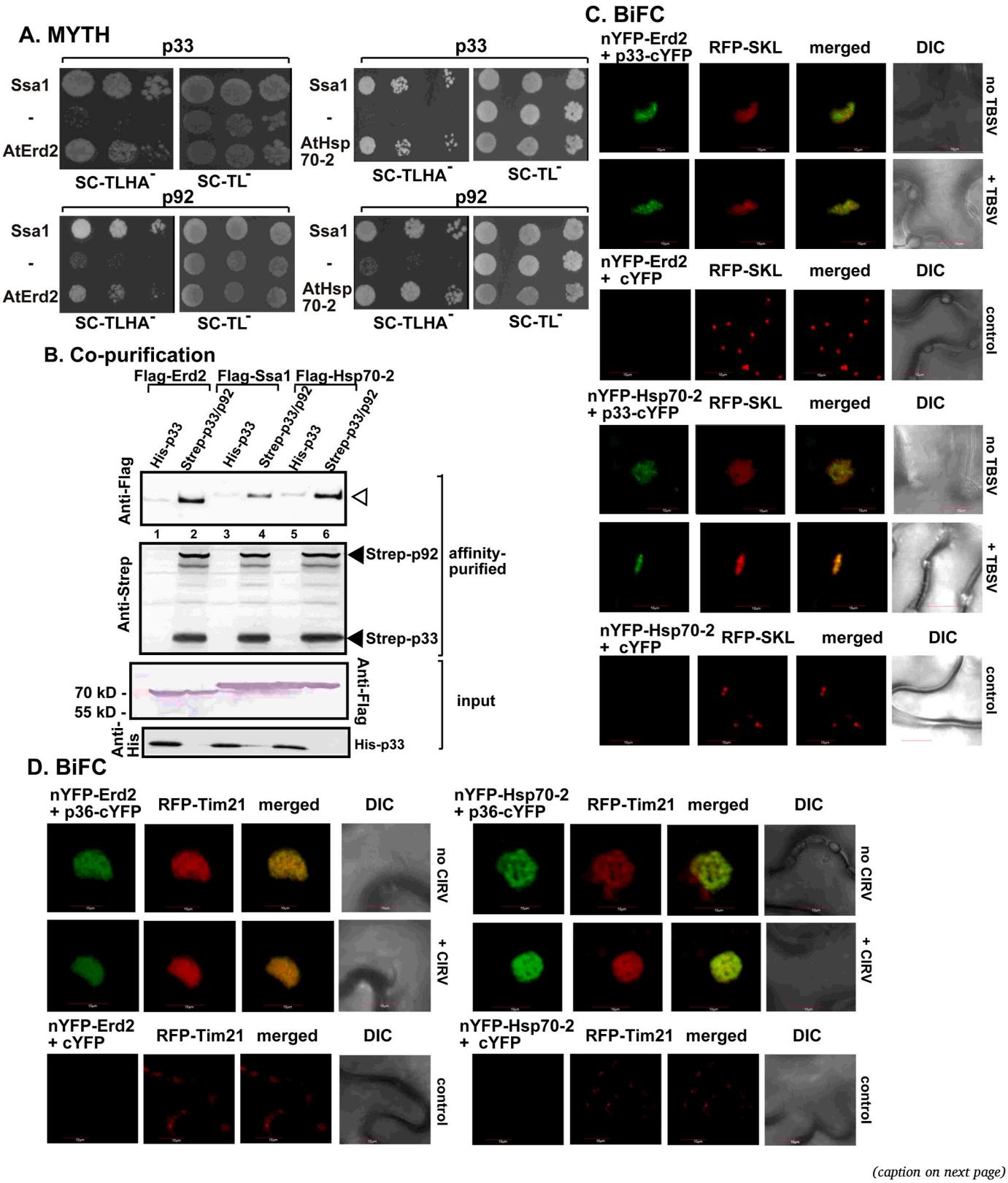

(caption on next page)

Fig. 1. The host AtErd2 and AtHsp70-2 are recruited into the tombusvirus replicase complex in yeast through interaction with the viral replication proteins. (A) The split-ubiquitin-based membrane yeast two-hybrid (MYTH) assay was used to show interaction between p33/p92 replication proteins and AtErd2 or AtHsp70-2 in yeast. The baits p33 or p92 were co-expressed with AtErd2 or AtHsp70-2 prey proteins. The yeast Ssa*1* (Hsp70 chaperone), and the empty prey vector (NubG) were used as positive and negative controls, respectively. (B) Co-purification of AtErd2 or AtHsp70-2 proteins with the 2xStrep-tagged p33 and 2xStrep-p92 replication proteins from the solubilized membrane fraction of yeast cells. Top panel: Western blot analysis of co-purified Flag-tagged cellular proteins with 2xStrep-affinity purified p33/p92. The Flag-tagged AtErd2 or and Flag-AtHsp70-2 proteins were detected with anti-Flag antibody. The negative control was His_6-tagged p33 from yeasts that was applied to a Strep-affinity column. Middle panel: Western blot of purified 2xStrep-p33 detected with anti-Strep antibody. Bottom panel: The total (input) expression levels of Flag-AtErd2, Flag-AtHsp70-2 or Flag-Ssa1 in yeasts are measured in total yeast extracts by western blotting using anti-Flag antibody. The experiments were repeated three times. (C) Interactions between TBSV p33-cYFP replication protein and the nYFP-AtErd2 or nYFP-AtHsp70-2 proteins were detected by BiFC. The merged images show the efficient co-localization of the peroxisomal RFP-SKL with the BiFC signal, indicating that the interactions between p33 replication protein and the co-opted host proteins take place within the large VROs. Scale bars represent 10 μm. (D) Interactions between CIRV p36-cYFP replication protein and the nYFP-AtErd2 or nYFP-AtHsp70-2 proteins were detected by BiFC within the VROs marked by the mitochondrial RFP-Tim21. Scale bars represent 10 μm. Each experiment was repeated three times.

Complementation with AtErd2 and AtHsp70–2 enhances tombusvirus replication in *ssa1Δssa2Δ* yeast. In the absence of the constitutively-expressed Ssa1 and Ssa2 (*ssa1Δssa2Δ* yeast), TBSV repRNA can only barely replicate in yeast, due to the partial complementation by the stress-inducible Ssa3 and Ssa4 Hsp70 proteins (Serva and Nagy, 2006; Wang et al., 2009). To demonstrate if the expression of AtErd2 and AtHsp70-2 can complement the defect in TBSV RNA replication in *ssa1Δssa2Δ* yeast, we analyzed TBSV repRNA accumulation 24 h after induction. Expression of either AtErd2 or AtHsp70-2 partially complemented TBSV repRNA replication in *ssa1Δssa2Δ* yeast (Fig. 3A and B). The complementation of CIRV replication by AtHsp70-2 was more pronounced than by AtErd2 in *ssa1Δssa2Δ* yeast (Fig. 3C and D). AtHsp70-2 rescued the accumulation of CIRV p36 replication protein, whereas AtErd2 did not in *ssa1Δssa2Δ* yeast (Fig. 3C and D), suggesting that different tombusviruses might subvert AtErd2 and AtHsp70-2 with different efficiencies.

Expression of AtErd2 and AtHsp70–2 in *N. benthamiana* enhances tombusvirus replication. To obtain further evidence on the pro-tombusviral functions of AtErd2 and AtHsp70-2, we transiently expressed them in *N. benthamiana* leaves infected with cucumber necrosis virus (CNV), a closely-related tombusvirus. The expression of AtErd2 or AtHsp70-2 increased CNV RNA accumulation by ~6 and 7-fold, respectively, 2.5 days after agroinfiltration (Fig. 4A and B), suggesting a strong pro-viral activity for AtErd2 and AtHsp70-2 in *N. benthamiana*. The plants expressing either AtErd2 or AtHsp70-2 showed more severe CNV-induced symptoms (5 dpi, Fig. 4C) and died more rapidly than CNV-infected plants agroinfiltrated with the empty vector (9 dpi, Fig. 4D). Mock-inoculated plants expressing either AtErd2 or AtHsp70-2 showed no phenotypes. Altogether, these experiments confirmed the pro-tombusviral activities of AtErd2 and AtHsp70-2 in plants.

Induction of Erd2-like Hsp70 expression in tombusvirus-infected *N. benthamiana* leaves. Since Erd2 homologues are not yet identified in *N. benthamiana*, we used Panther DB to search for a similar gene in *N. benthamiana* and *Solanum lycopersicum* databases. The Erd2-like gene from *N. benthamiana* and *S. lycopersicum* showed 86% and 85% similarity to AtErd2, respectively. Using qRT-PCR, we showed that the expression of Erd2-like Hsp70 was strongly induced in either TBSV or CIRV-infected *N. benthamiana* plants (Fig. 5). Also, when we used an antibody against Hsp70, then we observed 2-to-3-fold higher Hsp70 level in either TBSV or CIRV-infected *N. benthamiana* leaves (Fig. 6A). Also, semi-quantitative RT-PCR with Erd2 primers based on *N. benthamiana* or tomato sequences confirmed the induction of Erd2-like mRNAs during TBSV and CIRV infections of *N. benthamiana* (Fig. 6B). Altogether, these data suggest that the expression of Erd2-like Hsp70 and, in general, the accumulation of cytosolic Hsp70s is increased during tombusvirus infection of *N. benthamiana*. The higher Hsp70 level could be beneficial for tombusviruses due to need for these viruses to hijack Hsp70s to aid the infection process.

Knockdown of Erd2-like Hsp70 expression reduces tombusvirus replication in *N. benthamiana*. Knockdown of the canonical Hsp70-1 (and Hsp70-2 due to high sequence identity) via virus-induced gene silencing (VIGS) causes serious stunting and necrosis, followed by the death of *N. benthamiana* plants (Wang et al., 2009). Therefore, we focused on knocking down the *ERD2* gene expression here. We depleted the Erd2-like Hsp70 mRNA level by VIGS using the 3′ portion of the Erd2-like sequences cloned into a TRV-based vector in *N. benthamiana* (Fig. 7). Interestingly, the accumulation of the genomic RNAs of TBSV, CNV and CIRV tombusviruses greatly decreased in the inoculated leaves after VIGS treatment with Erd2-3' construct (Fig. 7). The knockdown plants stayed alive even after 10 days when the infected control plants died due to CNV or TBSV infections (Fig. 7C, E). Knockdown of Erd2-like sequences had only little effect on total Hsp70 protein levels on the 8th day of VIGS treatment (Fig. 7B) and the plants looked slightly stunted when compared with the control plants (Fig. 7E). In addition, knockdown of the Erd2-like Hsp70 also inhibited the accumulation of the more distantly-related red clover necrotic mosaic virus (RCNMV) in *N. benthamiana* (Fig. 7G).

Efficient *in vitro* activation of p92 RdRp by AtErd2 and AtHsp70–2. To demonstrate the similar biochemical functions of AtErd2 and the canonical AtHsp70-2 during TBSV replication, we performed *in vitro* experiments with purified proteins. First, we studied the ability of AtErd2 and AtHsp70-2 to activate the TBSV p92 RdRp. The freshly translated p92 RdRp is inactive prior to the assembly of the functional membrane-bound VRC. The RdRp activation step requires *cis*-acting elements in the viral (+)RNA, the p33 replication protein, subcellular membrane, and co-opted Ssa1/2 Hsp70 (Pogany and Nagy, 2012; Pogany et al., 2008). A simplified RdRp activation process was developed to test the requirement of host factors, mainly Hsp70 and phospholipids (Pogany and Nagy, 2015) (Fig. 8A). We have purified AtErd2 and AtHsp70-2 from yeast, and Ssa1 as a positive control (Fig. 8E), followed by the *in vitro* RdRp activation assay as depicted in Fig. 8A. Interestingly, both AtErd2 and AtHsp70-2 were able to support the RdRp activation step to an extent comparable to that of Ssa1 in case of AtErd2, whereas AtHsp70-2 was ~2-fold more efficient in this assay (Fig. 8B).

We also tested the function of AtErd2 or AtHsp70-2 in the assembly of the tombusvirus replicase *in vitro*, based on cell-free extract (CFE) prepared from yeast (Pogany et al., 2008). The purified recombinant p33 and $p92^{pol}$ replication proteins could only assemble replication-competent VRCs in the presence of yeast membrane fraction if functional Hsp70 is provided (Pogany and Nagy, 2012; Pogany et al., 2008). We found that the purified AtErd2 or AtHsp70-2 were able to support the assembly of the tombusvirus replicase *in vitro* (Fig. 8C and D). The efficiency of AtHsp70-2 was comparable to that of Ssa1 Hsp70 in the replicase assembly assay, while AtErd2 was ~3-fold less efficient (Fig. 8D). Altogether, the *in vitro* assays demonstrated that both AtErd2 and AtHsp70-2 could contribute to the assembly of the viral replicase and the activation of the viral RdRp *in vitro*, similar to the yeast Ssa1 Hsp70.

Allosteric Hsp70 inhibitors block the assembly of the tombusvirus replicase complex *in vitro*. The emerging conclusion from the above data and previous works (Pogany and Nagy, 2015; Pogany et al., 2008; Wang et al., 2009; Wang et al., 2009a,b) is that several cytosolic

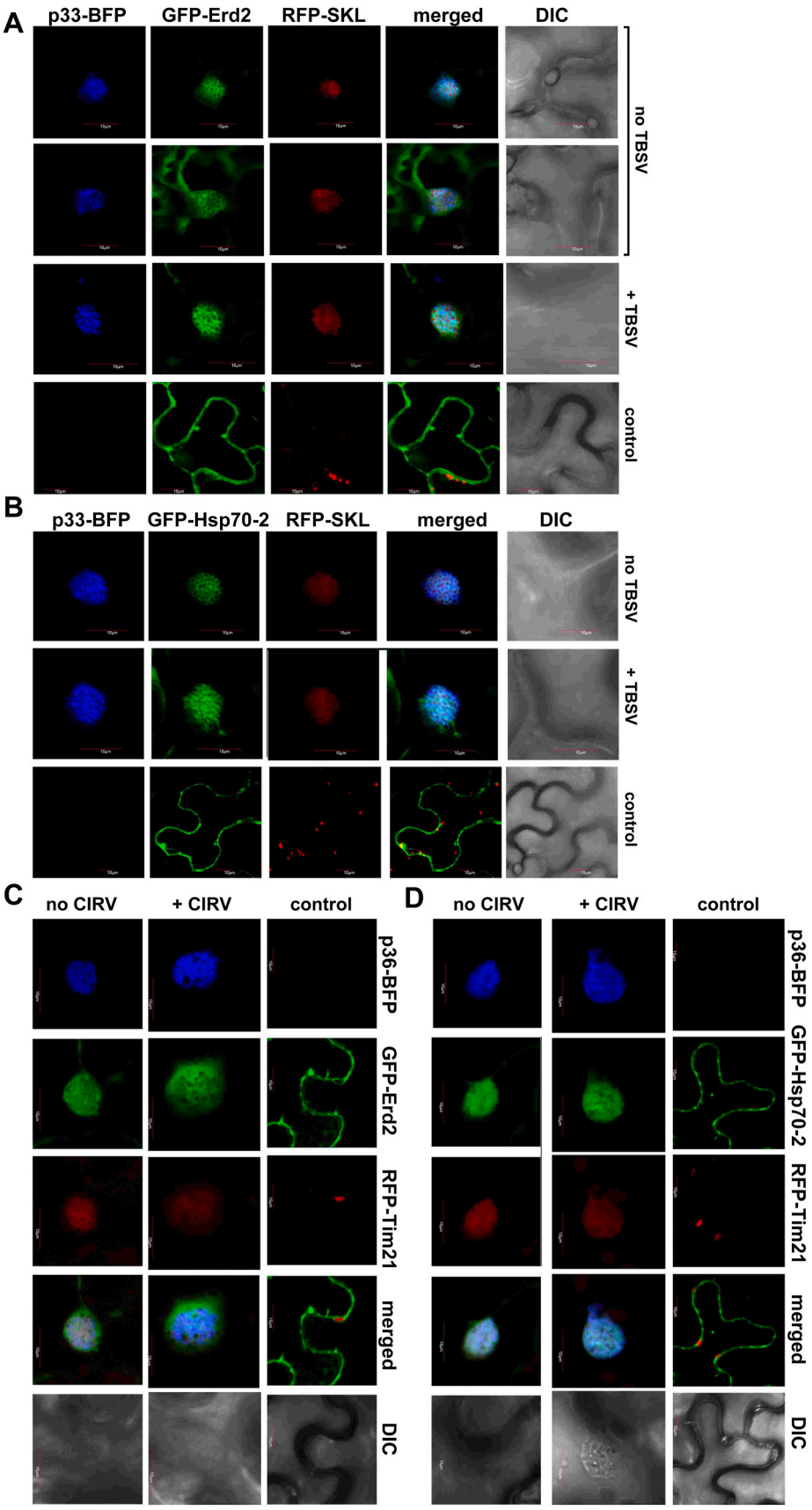

Fig. 2. Re-targeting of host AtErd2 and AtHsp70–2 into the TBSV and CIRV VROs in *N. benthamiana*. (A–B) Confocal microscopy images show efficient co-localization of TBSV p33-BFP replication protein and the GFP-AtErd2 (panel A) or GFP-AtHsp70-2 (panel B) proteins within VROs marked by RFP-SKL peroxisomal marker in *N. benthamiana* leaves. Expression of these proteins from the 35S promoter was done after co-agroinfiltration into *N. benthamiana* leaves. The plant leaves were either TBSV-infected or mock-inoculated as shown. Scale bars represent 10 μm. (C–D) Confocal microscopy images show efficient co-localization of CIRV p36-BFP replication protein and the GFP-AtErd2 (panel C) or GFP-AtHsp70-2 (panel D) proteins within VROs marked by RFP-Tim21 mitochondrial marker in *N. benthamiana* leaves. The plant leaves were either CIRV-infected or mock-inoculated as shown. See further details in panel A–B. Each experiment was repeated three times.

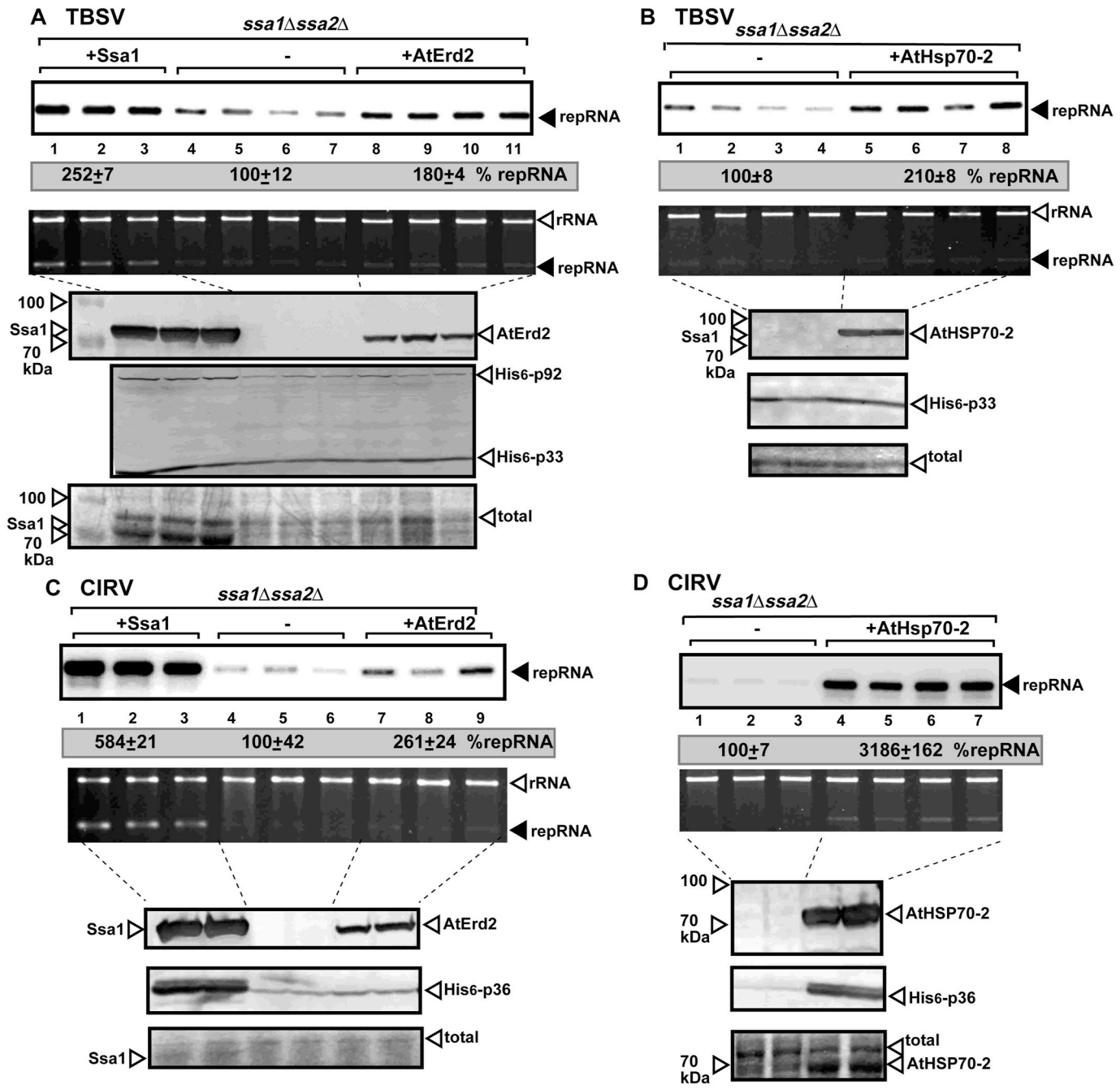

Fig. 3. Complementation assay through expression of AtErd2 or AtHsp70-2 shows increased TBSV and CIRV accumulation in *ssa1Δssa2Δ* yeast. (A–B) Top image: Northern blotting of TBSV repRNA accumulation in *ssa1Δssa2Δ* yeast. The yeasts co-expressed the tombusvirus His_6-p33 and His_6-p92 replication proteins and the TBSV DI-72 repRNA with Flag-tagged Ssa1, Flag-AtErd2 or Flag-AtHsp70-2 from plasmids for 24 h at 23 °C. The accumulation level of repRNA was measured using ImageQuant software. Ribosomal RNA was used as a loading control (see middle panel). Bottom images: Western blotting shows the accumulation levels of Flag-Ssa1, Flag-AtErd2 or Flag-AtHsp70-2 and His_6-p33 with His_6-p92 in the above yeast samples. Coomassie-blue-stained SDS-PAGE shows total protein loading. Note that the yeast Ssa1 or AtHsp70-2 is visible in some total protein samples. (C–D) Similar assays are shown as in panels A and B, except we expressed the CIRV His_6-p36 and His_6-p95 replication proteins to support repRNA replication. The experiments were repeated three times.

Hsp70 family members are co-opted by tombusviruses to support replication and Hsp70s could emerge as possible targets for antiviral approaches. There are major on-going efforts to develop Hsp70 inhibitors to treat various genetic and tumor-related diseases (Li et al., 2015; Pratt et al., 2014; Zuiderweg et al., 2013). Therefore, we decided to test allosteric Hsp70 inhibitors to control tombusviruses in cell-free replicase reconstitution assay (see below).

Because Hsp70 goes through conformational change upon binding to either ATP or ADP, it is possible to target the allosteric forms of Hsp70, instead of the catalytic site by small molecule drugs (Assimon et al., 2013; Evans et al., 2010; Rousaki et al., 2011; Zuiderweg et al., 2013). The advantage of the allosteric approach that it has wide range of inhibition on all Hsp70s expressed from multicopy genes in a particular host due to the conserved sequences in the targeted regions. We have tested seven membrane permeable small molecule compounds from Dr. Jason Gestwicki (UCSF). The first class of inhibitors is MKT-077 and its derivatives, which include MKT-077, YM-01, JG-40, JG-48, and JG-98. These chemicals bind to the Hsp70-ADP form, but not to the

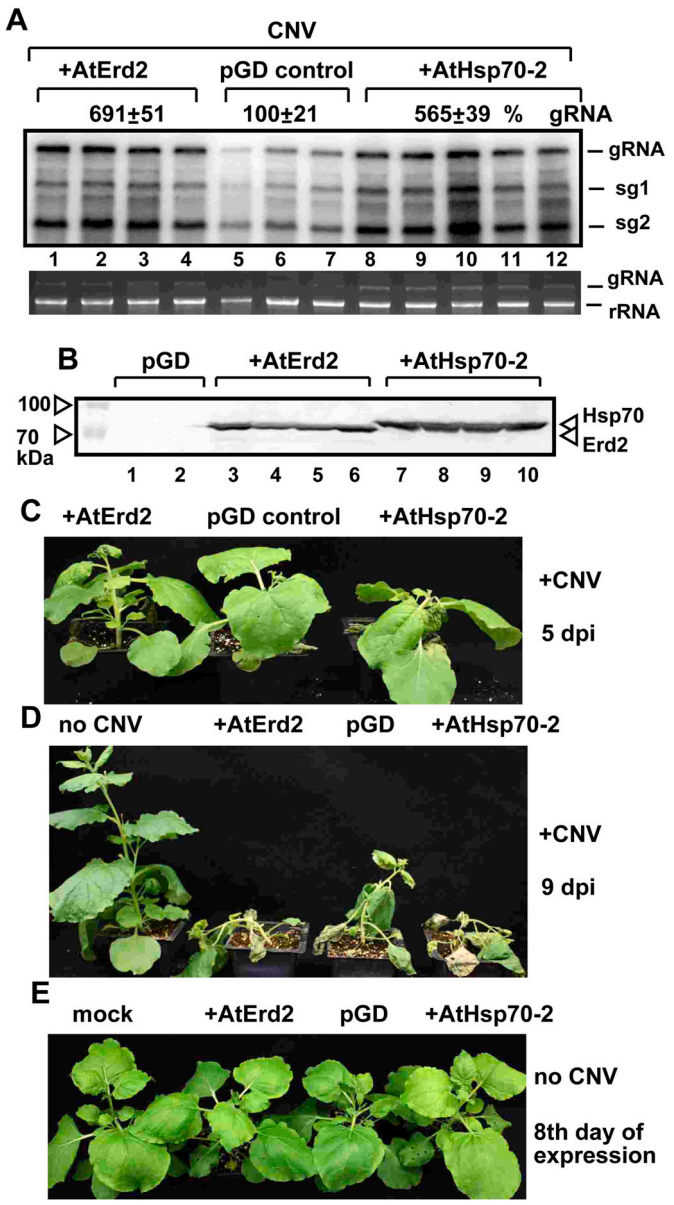

Fig. 4. Expression of AtErd2 or AtHsp70-2 enhances CNV RNA accumulation in *N. benthamiana*. (A) Northern blot analysis of CNV genomic (+)RNA, subgenomic RNA1 and sgRNA2 accumulation in *N. benthamiana* expressing AtErd2 and AtHsp70-2 from plasmids. The plants were inoculated with CNV virion preparation one day after agroinfiltration. Samples were taken 2.5 dpi. Note that all the plant leaves co-expressed the TBSV p19 RNA silencing suppressor. Ribosomal RNA visualized by ethidium-bromide staining in agarose gels is shown as a loading control. Note that the genomic RNA could be seen in several samples, showing high CNV accumulation. Each experiment was repeated at least three times. (B) Western blotting shows the accumulation levels of Flag-AtErd2 or Flag-AtHsp70-2 in the above plant samples. (C–E) Images of CNV-infected or mock-inoculated *N. benthamiana* plants expressing AtErd2 or AtHsp70-2 or the empty pGD plasmid as a control. Note the appearance of more intense CNV symptoms when AtErd2 or AtHsp70-2 is expressed. (E) The lack of phenotype on *N. benthamiana* expressing AtErd2 and AtHsp70-2 from plasmids eight days after agro-infiltration. The mock plants were infiltrated with buffer only. Each experiment was repeated three times.

Hsp70-ATP form (Gestwicki and Shao, 2019; Rousaki et al., 2011; Zuiderweg et al., 2013). The binding of these allosteric inhibitors limits ATPase activity and stabilizes the Hsp70-substrate complex, altering the dynamics of the substrate release and promoting substrate degradation by the proteasome. Another inhibitor, CE-12, inhibits the ATPase activity of Hsp70 (Chafekar et al., 2012). On the other hand, 115-7c inhibitor stabilizes the Hsp70-ATP form, thus reducing the ability of Hsp70s to bind stably to the substrate.

To test if viral replication could be affected by the various allosteric Hsp70 inhibitors, we used *in vitro* approaches. First, we tested the effectiveness of allosteric Hsp70 inhibitors to block the assembly of the tombusvirus replicase in a cell-free yeast extract (CFE) and purified recombinant TBSV replication proteins (Fig. 9A) (Pogany et al., 2008). All the tested compounds strongly inhibited TBSV replication *in vitro* (Fig. 9B). MKT-077, YM-01, JG-40 and JG-98 were effective inhibitors of TBSV replication *in vitro* even at low concentrations (Fig. 9C). These data confirm the direct inhibitory effects of these compounds on the activity of the TBSV replicase *in vitro*.

The second test included the TBSV RdRp activation assay, which requires Hsp70 function to make a truncated recombinant p92 as a functional RdRp (Pogany and Nagy, 2012, 2015). Addition of increasing amounts of the inhibitory compounds to the RdRp activation assay revealed that six of the allosteric Hsp70 inhibitors were potent in blocking the RdRp activity of p92 replication protein (Fig. 9D). The most probable explanation is that the allosteric Hsp70 inhibitors blocked the function of Hsp70 (present in the soluble fraction of yeast CFE) in activating p92 RdRp *in vitro*. Altogether, we found that these allosteric inhibitors, in spite of their different activities, inhibited TBSV replicase activity likely due to blocking Hsp70 functions needed for TBSV replication.

Allosteric Hsp70 inhibitor YM-01 reduces TBSV replication in yeast cells. To test the *in vivo* effectiveness of the allosteric Hsp70 inhibitors in blocking TBSV replication, we decided to continue working with YM-01 inhibitor, which represents the first class of inhibitors and it was highly effective in the *in vitro* work above. First, we have applied YM-01 to yeast cultures in increasing concentrations, which resulted in inhibition of TBSV repRNA accumulation by up to ~90% with 100 μM showing the strongest inhibition (Fig. 10A). YM-01 also inhibited the accumulation of the TBSV p33 replication protein in yeast (Fig. 10A). These experiments confirmed that an allosteric inhibitor of the cellular Hsp70 has strong anti-TBSV activities in yeast.

One of the major functions of the co-opted Hsp70 in tombusvirus replication is the facilitation of membrane-association of the tombusvirus replication proteins, which is critical for the functional VRC assembly (Wang et al., 2009; Wang et al., 2009a,b). Partial inactivation of a temperature-sensitive *ssa1*^{ts} in the absence of *SSA2-4* led to mostly cytosolic distribution of the tombusvirus p33 replication protein (Wang et al., 2009; Wang et al., 2009a,b). To test if the allosteric Hsp70 inhibitor YM-01 could interfere with the membrane association of the tombusvirus replication protein, we used confocal laser microscopy with a functional YFP-tagged p33 in yeast treated with YM-01 or DMSO as a negative control (Fig. 10B and C). Interestingly, treatment of yeast with YM-01 delayed the membrane-(peroxisome-) association of YFP-p33 by 4-to-8 hours when compared with the DMSO-treated control yeast cells (Fig. 10B and C). At a latter time point (24 h), however, the YFP-p33 was present in punctate structures (several of those co-localized with the peroxisomal Pex13-CFP marker protein), indicative of localization of YFP-p33 to the peroxisomes in YM-01-treated yeast at the late time point (Fig. 10B and C).

Allosteric Hsp70 inhibitors reduce tombusvirus replication in plant cells. To test if allosteric Hsp70 inhibitors could also affect the replication of the full-length tombusvirus in plant cells, first we tested the effective concentration of MKT-077 and YM-01 in *N. benthamiana* protoplasts electroporated with the TBSV genomic (g)RNA. We separately applied 100 μM of MKT-077 and YM-01 to *N. benthamiana* protoplasts electroporated with TBSV RNA. Northern blot analysis of the TBSV RNA 24 h after electroporation into plant protoplasts revealed strong reduction in TBSV RNA accumulation reaching up to 90–95% decrease in virus accumulation (Fig. 11A). Altogether, the plant protoplasts experiments strongly supported most of the findings obtained *in vitro* assays and with yeast on the inhibitory effects of these allosteric

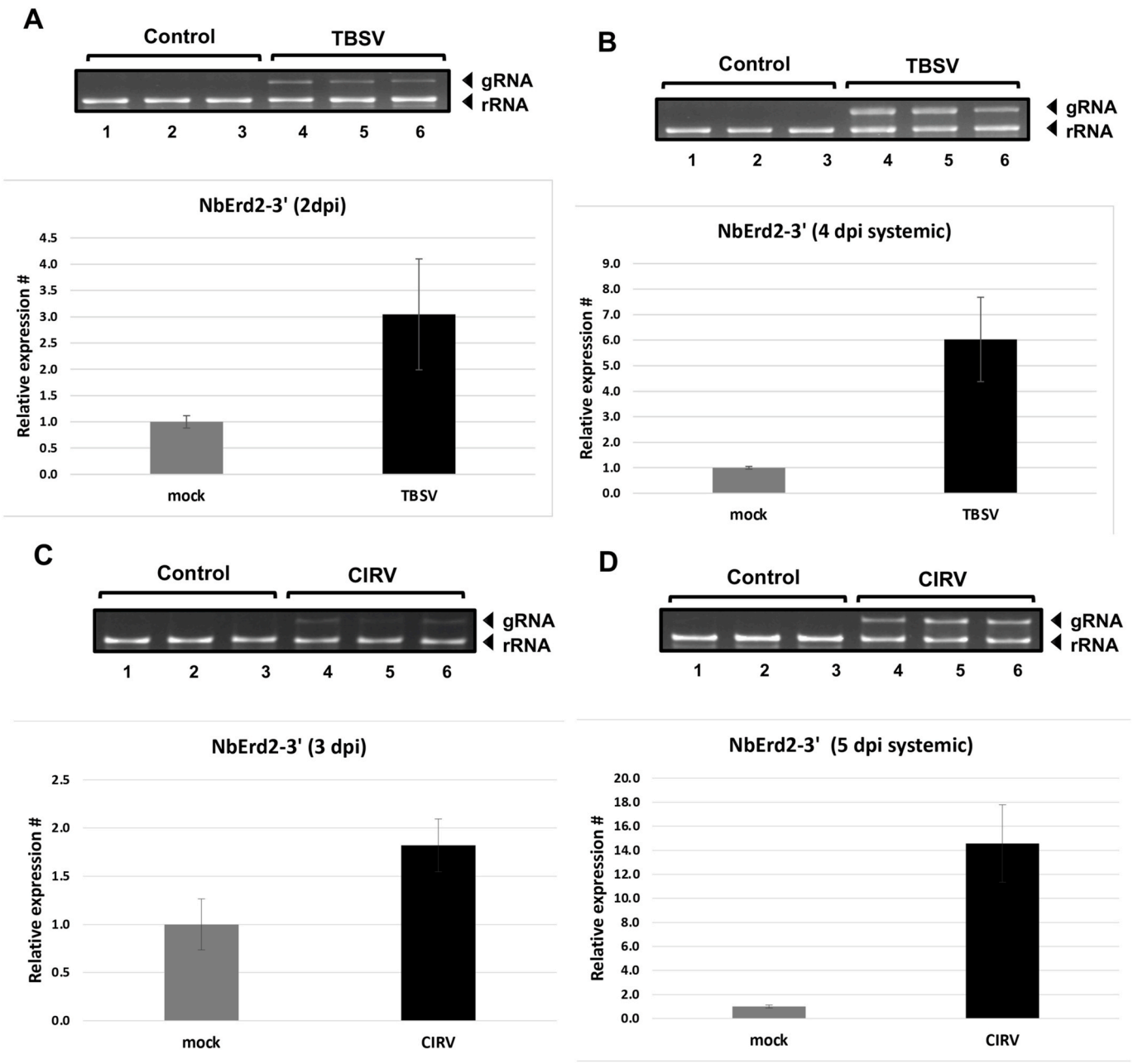

Fig. 5. Quantitative RT-PCR analysis of Erd2 mRNA expression in tombusvirus-infected *N. benthamiana* leaves. (A–B) Top images: Total RNA samples from mock-inoculated or TBSV-infected plants are visualized by ethidium-bromide staining of agarose gel as loading controls. Total RNA samples were from the inoculated leaves (panel A) or from the TBSV-systemically-infected leaves (panel B). Note that both the ribosomal RNA and the TBSV genomic RNA are seen in samples, showing high virus accumulation. Quantitative RT-PCR shows the Erd2 mRNA levels based on 3′ sequences. Each experiment was repeated at least three times. Note that the NbErd2 sequence was obtained based on sequence comparison with AtErd2. (C–D). Comparable experiments based on CIRV. Please find details in panel A–B.

Hsp70 inhibitor compounds on TBSV replication.

To test if selected allosteric Hsp70 inhibitors also affect the replication of other viruses, first we compared the effects of various concentrations of YM-01 on CNV and CIRV accumulation in plant protoplasts. YM-01 showed high efficiency in inhibition of tombusvirus accumulation in a concentration-dependent fashion in protoplasts (Fig. 11B and C). Similarly to yeast, YM-01 also inhibited the accumulation of the p33 replication protein in plant protoplasts (Fig. 11B).

To test a more distantly related plant virus, we studied turnip crinkle virus (TCV), which belongs to carmoviruses in the Tombusviridae family. TCV accumulation was inhibited by YM-01 in *N. benthamiana* protoplasts (Fig. 11D).

Allosteric Hsp70 inhibitors reduce TBSV replication in plants. The extend our above findings to plants, we infiltrated the allosteric Hsp70 inhibitors into *N. benthamiana* plant leaves infected with TBSV. Northern blot analysis of total RNA extracts from the leaves infiltrated either with either MKT-077 or YM-01 revealed the extensive inhibition of TBSV RNA accumulation (Fig. 12A and B). YM-01 also reduced TCV RNA accumulation in the infiltrated *N. benthamiana* leaves (Fig. 12E).

Finally, we also tested JG-98 inhibitor in plants, because it was the most potent inhibitor of TBSV replicase activity *in vitro* (Fig. 9). We found that treatment with JG-98 inhibitor strongly decreased TBSV and CIRV RNA accumulation in *N. benthamiana* leaves (Fig. 12C and D). Altogether, these data suggest that the allosteric Hsp70 inhibitors are effective against selected plant RNA viruses in plants. We did not observe any detrimental effects caused by treatment with these Hsp70

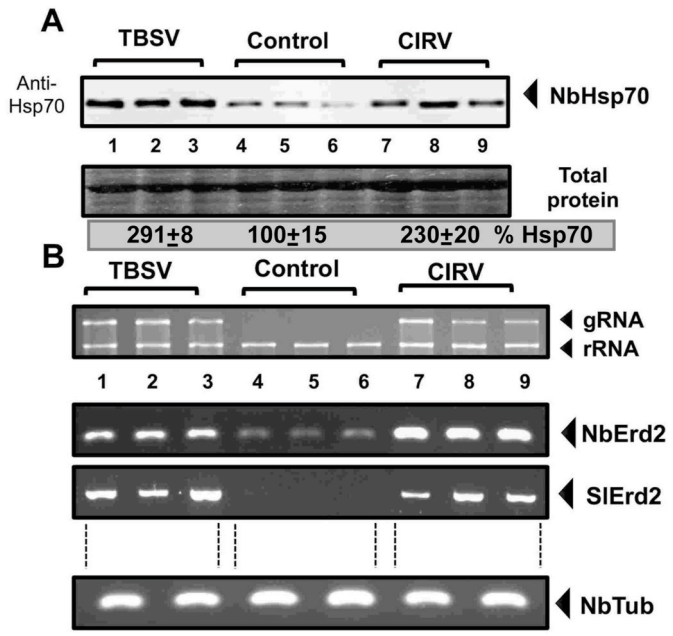

Fig. 6. Induction of Erd2 and Hsp70 expression in tombusvirus-infected *N. benthamiana* leaves. (A) Western blotting of total protein extracts shows increased accumulation of NbHsp70 using anti-Hsp70 antibody in plant samples obtained from either TBSV or CIRV-infected or mock-inoculated plants. Total protein extracts are shown in a Coomassie blue-stained SDS-PAGE as protein loading controls. (B) Top image: Ribosomal RNAs in total RNA samples visualized by ethidium-bromide stained agarose gel are shown as loading controls. Note that the tombusvirus genomic RNA could be seen in samples, showing high virus accumulation. Middle images: Semi-quantitative RT-PCR to measure NbErd2 mRNA levels in TBSV or CIRV-infected plants 4 dpi in case of TBSV and 5 dpi in case of CIRV versus the mock-treated plants. Note that the RT-PCR primers for the NbErd2 sequence were designed based on sequence comparison with AtErd2 (second panel). In the third panel, we used primers based on the related *S. lycopersicum* Erd2 sequences for the RT-PCR analysis of the same total RNA samples. Bottom image: Semi-quantitative RT-PCR of tubulin mRNA in the above samples, as controls. The experiments were repeated three times.

inhibitors on the control, uninfected leaves, likely due to timely degradation of the inhibitors.

Allosteric Hsp70 inhibitors reduce nodavirus replication in yeast. We also tested the effect of YM-01 on two insect (+)RNA nodaviruses, FHV and Nodamura virus (NoV), which are unrelated to tombusviruses, in yeast cells replicating the RNA1 component (Fig. 13). Interestingly, the replication of RNA1 and synthesis of subgenomic RNA3 from the RNA1 template were strongly inhibited by YM-01 (Fig. 13A–C). Overall, these data strongly support the model that inhibition of Hsp70 functions by allosteric inhibitors has strong antiviral effects on multiple (+)RNA viruses at the single cell level.

3. Discussion

The large number of viruses infecting humans, animals and plants code for specialized viral proteins adapted to their hosts, thus presenting a major challenge to develop broad-range antiviral strategies. However, viruses need to co-opt host proteins to support their replication and infection. These host proteins could provide "universal" and broad-range antiviral targets to inhibit their pro-viral functions and thus, interfere with infections caused by many different viruses or even other pathogens. The hosts' Hsp70s might represent one of those targets for antivirals due to their wide-spread hijacking by numerous viruses and pathogens. Indeed, the role of Hsp70 chaperones in replication was documented for several flaviviruses (Bozzacco et al., 2016; Taguwa et al., 2015, 2019), influenza virus (Cao et al., 2014; Manzoor et al., 2014), and several plant viruses (Chenon et al., 2012; Lamm et al., 2017; Lohmus et al., 2017; Nagy et al., 2011; Verchot, 2012; Wang et al., 2018).

Hsp70 family members are molecular chaperones that are involved in maintaining cellular homeostasis from bacteria to humans (Patury et al., 2009; Wang et al., 2013; Zuiderweg et al., 2017). Small chemical inhibitors of Hsp70s have been identified (Assimon et al., 2013; Cesa et al., 2013; Evans et al., 2010; Patury et al., 2009), and these inhibitors act only for a limited time, allowing the survival of the host.

Accordingly, we have demonstrated here that different classes of allosteric inhibitors of Hsp70s greatly inhibited the replication of TBSV *in vitro*. The most potent inhibitors belong to the MKT-077 class, which limits ATPase activity of Hsp70. This class of allosteric inhibitors of Hsp70 blocked TBSV replicase assembly and the activation of the RdRp function of $p92^{pol}$ replication protein. Two other types of allosteric inhibitors with different mode of action were less inhibitory on TBSV replicase assembly and RdRp activation. Overall, the biochemical and cellular assays revealed that multiple functions of the co-opted Hsp70 in TBSV replication could be blocked by allosteric inhibitors of Hsp70s. Experiments in yeast and plants confirmed that the MKT-077 class of allosteric inhibitors have a great potential as antiviral compounds against a group of plant and insect (+)RNA viruses.

Several members of the large Hsp70 protein family are hijacked by tombusviruses for multiple pro-viral functions (Pogany and Nagy, 2015; Pogany et al., 2008; Wang et al., 2009; Wang et al., 2009a,b). These members include the cytosolic Ssa1/2 in yeast and the plant AtHsp70-1, AtHsp70-2 and AtErd2 that interact with the TBSV p33 replication protein (Molho et al., 2021; Serva and Nagy, 2006). In this paper, we provide biochemical evidence that AtErd2 and AtHsp70-2 of the plant Hsp70 family perform comparable pro-viral functions to the previously characterized yeast Ssa1 and Ssa2 cytosolic Hsp70s in TBSV replication (Pogany and Nagy, 2015; Pogany et al., 2008; Wang et al., 2009; Wang et al., 2009a,b). The purified recombinant AtErd2 and AtHsp70-2 were found to activate the RdRp function of $p92^{pol}$, which was capable to synthesize complementary RNA in the presence of one of these Hsp70s. Moreover, the low level of TBSV repRNA replication in the yeast CFE membrane fraction was greatly boosted by the addition of purified recombinant AtErd2 and AtHsp70-2, similar to the yeast Ssa1. All these *in vitro* data firmly establish the equivalent pro-viral functions for AtErd2 and AtHsp70-2 and the yeast Ssa1/2 in TBSV replication.

Additional functional evidence for the pro-viral functions of AtErd2 and AtHsp70-2 was obtained in yeast missing *SSA1/2* by showing the ability of AtErd2 and AtHsp70-2 to complement TBSV repRNA replication. In addition, co-purification experiments showed the presence of AtErd2 and AtHsp70-2 in the affinity-purified viral replicase preparation. The recruitment of AtErd2 and AtHsp70-2 into the VRCs likely accomplished by the direct interaction between AtErd2 and AtHsp70-2 and the p33 replication protein, which constitutes the most abundant component of the VRCs. Interestingly, AtErd2 and AtHsp70-2 play similar functions for CIRV, a tombusvirus, which replicates in the outer mitochondrial membrane instead of the peroxisomal membrane as in the case of TBSV and CNV (Panavas et al., 2005a; Weber-Lotfi et al., 2002; Xu et al., 2012).

The expression of AtErd2 and AtHsp70-2 in *N. benthamiana* has increased tombusvirus replication, suggesting that these Hsp70s are limiting factors in plants. Similar to the inhibitory effects on TBSV by the allosteric Hsp70 inhibitors, knocking down Erd2 Hsp70 hindered tombusvirus (TBSV, CNV and CIRV) replication in *N. benthamiana*. Moreover, we obtained evidence that the expression of Erd2 and other Hsp70s are up-regulated in tombusvirus-infected N. *benthamiana*. The increased Hsp70 level in tombusvirus-infected *N. benthamiana* was also demonstrated by western blotting using plant Hsp70 monoclonal antibody. Our results confirm the findings of Alam and Rochon, who demonstrated increased accumulation of Hsp70s in *N. benthamiana* infected with CNV (Alam and Rochon, 2015).

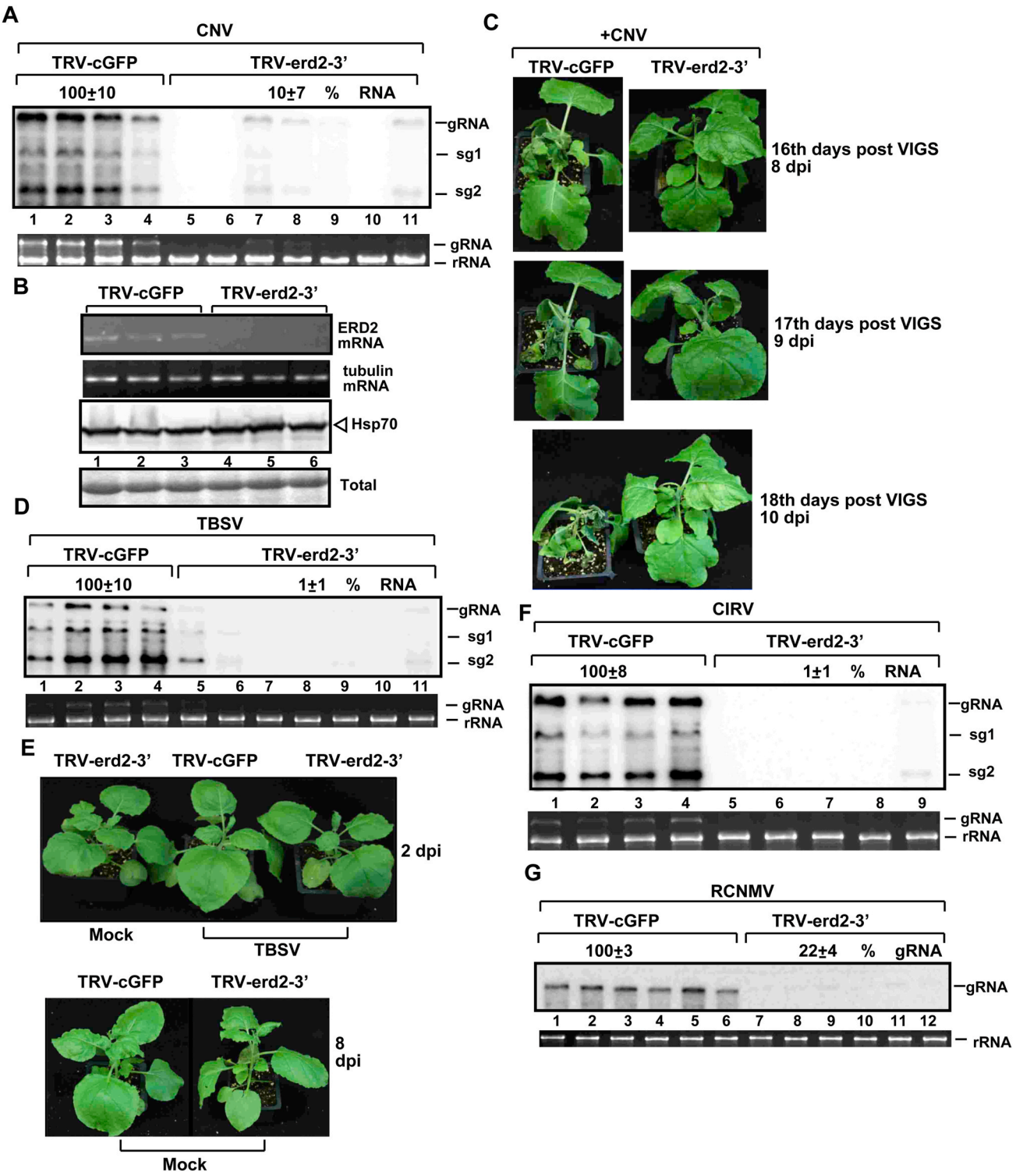

Fig. 7. Knockdown of Erd2 reduces tombusvirus RNA accumulation in *N. benthamiana*. (A) Accumulation of CNV genomic RNA in NbErd2 knockdown *N. benthamiana* plants 2.5 d post-inoculation, based on Northern blot analysis of total RNA samples. Note that we used a CNV lacking the p20 silencing suppressor (called $CNV^{20KSTOP}$). VIGS was performed via agroinfiltration of TRV vectors carrying *NbERD2*- 3′ sequence (TRV-erd2-3′) or the TRV-cGFP vector (as a control). Inoculation with CNV gRNA was done 8 days after agroinfiltration (dpa). (B) Semi-quantitative RT-PCR was used to measure the knockdown of Erd2 mRNA in plants 8 days after agroinfiltration. Middle image: Semi-quantitative RT-PCR of the tubulin mRNA in the above samples, as controls. Bottom image: Western blot of the total protein extracts shows the levels of NbHsp70s using anti-Hsp70 antibody in the above plant samples. (C) Inhibition of CNV-induced symptom development in *NbERD2* knockdown *N. benthamiana*. Note the reduced severity of symptoms caused by CNV in the *NbERD2* knockdown plant when compared with the rapidly developing lethal necrosis in the control plants. (D) Accumulation of TBSV genomic RNA in *NbERD2* knockdown *N. benthamiana* plants 2 d post-inoculation, based on northern blot analysis. Find further details in panel A. (E) Inhibition of TBSV-induced symptom development in *NbERD2* knockdown *N. benthamiana*. Find further details in panel C. (F) Accumulation of CIRV genomic RNA in *NbERD2* knockdown *N. benthamiana* plants 3 dpi, based on northern blot analysis. Find further details in panel A. (F) Accumulation of Red clover necrotic mosaic virus (RCNMV, distantly-related to TBSV) genomic RNA1 in *NbERD2* knockdown *N. benthamiana* plants 6 dpi, based on northern blot analysis. See additional details in panel A. Each experiment was repeated at least three times.

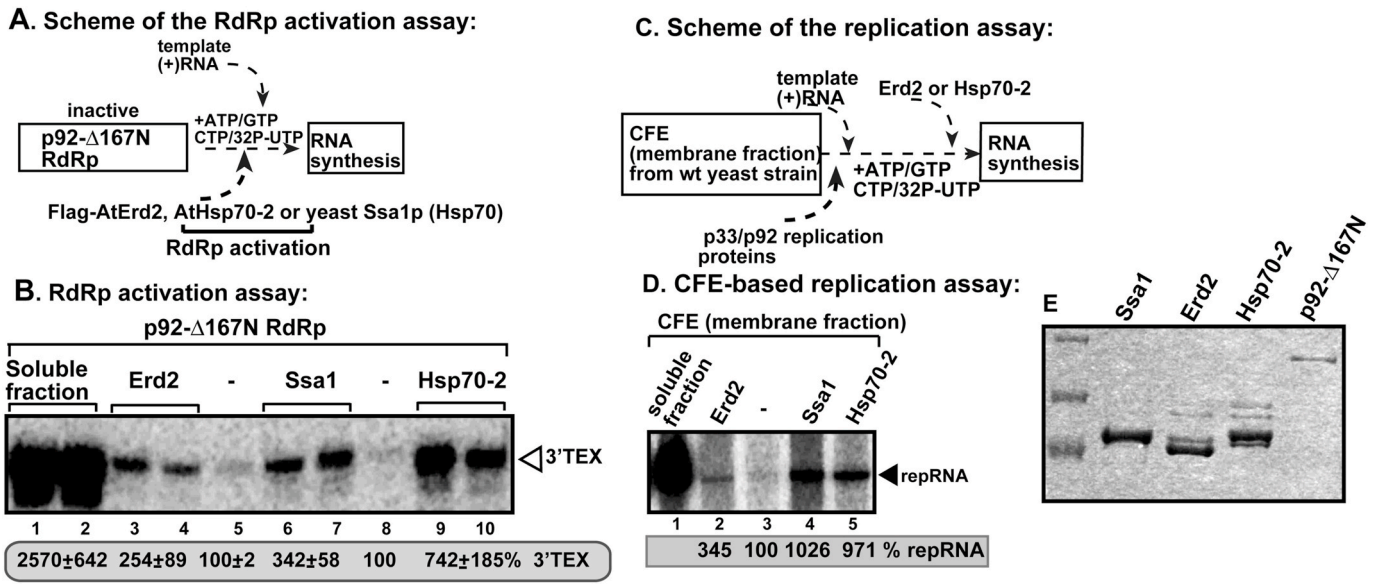

Fig. 8. Stimulation of *in vitro* activation of TBSV RdRp function by AtErd2 and AtHsp70-2. (A) Scheme of the *in vitro* RNA synthesis assay with DI-mini (+)RNA and purified recombinant p92-Δ167N TBSV RdRp protein and the added Hsp70 derivatives. The activation of recombinant p92-Δ167N RdRp protein leads to the production of a 3′-terminal extension (3′-TEX) product. (B) Denaturing PAGE analysis of the ^{32}P-labeled RNA products obtained in an *in vitro* assay with the activated recombinant p92-Δ167N RdRp. The samples contained the FLAG-affinity-purified AtErd2, AtHsp70-2 or Ssa1p Hsp70 proteins (13 pmol) or DMSO. The soluble fraction containing Ssa1 and Ssa2 Hsp70 was prepared from WT yeast using centrifugation to remove the membrane fraction. The amounts of 3′TEX products were estimated using the ImageQuant software. (C) Scheme of the CFE-based TBSV replicase reconstitution assay. The membrane fraction of yeast CFE was programmed with *in vitro* transcribed TBSV DI-72 (+)repRNA and purified recombinant MBP-p33 and MBP-p92^{pol} replication proteins of TBSV. Comparable amounts of FLAG-affinity-purified AtErd2, AtHsp70-2 or Ssa1p Hsp70 proteins were added to the assay. (D) Denaturing PAGE analysis of the ^{32}P-labeled TBSV repRNA products obtained in the CFE-based TBSV replicase reconstitution assay. repRNA production was measured using ImageQuant software. Lane 1 contains the soluble fraction of yeast CFE, containing Ssa1 and Ssa2 Hsp70s. The experiments were repeated three times. (E) SDS-PAGE analysis shows the quality of the purified Flag-AtErd2, Flag-AtHsp70-2 or Flag-Ssa1 Hsp70 proteins (from yeast) and the MBP-tagged p92-Δ167N RdRp (from *E. coli*). The experiments were repeated three times.

Allosteric inhibitors of host Hsp70s were also effective against Dengue virus (DENV), hepatitis C virus and other flaviviruses (Khachatoorian et al., 2016; Taguwa et al., 2015). These inhibitors inhibited DENV replication and packaging, and they also affected host responses, such as proinflammatory cytokines. Importantly, cytotoxicity of these inhibitors was negligible in human cells (Khachatoorian et al., 2016; Taguwa et al., 2015). Therefore, allosteric inhibitors of host Hsp70s are promising as broad-spectrum antivirals in plants and animals.

4. Materials and methods

Yeast strains. The wt yeast (*Saccharomyces cerevisiae*) strain BY4741 (*MATa his3Δ1 leu2Δ0 met15Δ0 ura3Δ0*) was obtained from Open Biosystems. NMY51 [*MATa his3Δ 200 trp1-901 leu2-3, 112 ade2 LYS2*:(*lexAop*)$_4$-*HIS3 ura3*:(*lexAop*)$_8$-*lacZ ade2*:(*lexAop*)$_8$-*ADE2 GAL4*] was obtained from Dualsystems. Double mutant yeast *ssa1 ssa2* strain, MW123 (his3 leu2 lys2 trp1 ura3 ssa1:HIS3 ssa2:LEU2) was provided by Elizabeth A. Craig (University of Wisconsin) (Becker et al., 1996).

Yeast and plant plasmids. To construct yeast plasmids pRS315-Nflag-AtErd2, pRS315-Nflag-ssa1, pRS315-Nflag-AtHsp70-2, *AtERD2* exon1 and exon2 were PCR-amplified using *A. thaliana* genomic DNA with primers #5643 (CCGGGATCCATGGCTGGTAAGGGAGAAG) and #5644 (CGAAAACGGTGTTAACAGGGTTC) and #5645 (GAACCCTGTTAACACCGTTTTCGACGCAAAGAGGTTGATTGGTC G) and #5646 (CCGCTCGAGTCAGCTAGCTCCTTGATACATCTTAGTG). The final *ERD2* product was amplified by overlapping PCR with primers #5643–5646 and digested with *Bam*HI and *XhoI*. Ssa1 (hsp70) was cloned from yeast cDNA with primers #2030 (CGCGGGATCCATGTCAAAAGCTGTCGGTATTG) - #2812 (GGCCTCGAGTTAATCAACTTCTTCAACGGTTGG), as previously described (Wang et al., 2009) and digested with *Bam*HI and *XhoI*. *At*Hsp70-2 were cloned using cDNA from *A. thaliana* via performing nested PCR with primers #6247 (CCTAGCTCTATTCTTTCTCTTTGCTGC) and #6248 (GAGAAAGGGGTCACCAATGACC), followed by another PCR-amplification with primers #6302 (CCGCCCGGGATGGCTGGTAAAGGAGAAGGTCC) and #6252 (CCGCTCGAGTTAGTCGACTTCCTCGATCTTG) and the obtained PCR product was digested with *XmaI* and *XhoI*. The obtained products were inserted into pRS315-Nflag digested with *Bam*HI and *XhoI* or *Xma* and *SalI*, respectively.

To generate plasmid pRS317-TET-p95, pCM189 plasmid containing TET promoter was digested with *EcoRI* and *PstI* and ligated into pRS317 vector digested with *EcoRI* and *PstI*. The CIRV p95 gene sequence was PCR-amplified with primers #6245 (GCACGGCCGATGGATTACAAGGACGATGACGATAAGGTACCC) and #6246 (GCAGCGGCCGCATGCAGCTGGATCTTCGAG), digested with *Eco521* and *NotI* and cloned into the pRS317-TET vector digested with *Eco521* and *NotI*. The direction of the insert was verified by restriction enzyme digestions.

To generate plasmid pESC-Trp-Cup, the CUP1 promoter was PCR-amplified using primers #2741 (CCGCGAGCTCCATTACCGACATTTGGGCGCTA) and #2594 (CGCGCTCGAGAATTCGTTACAGTTTGT). The obtained PCR product was digested with *Sac1* and *XhoI* and ligated intto pESC-Trp vector. *AtERD2*, *AtHsp70-2,* and *SSA1* sequences were cloned following the strategies mentioned above using PCR with primers #5643 and 5646 (*Bam*HI and *XhoI*), #2030 and #2812 (*Bam*HI and *XhoI*), and #6249 (CCGCTCGAGATGGATTACAAGGACGATGACGATAAGGCTGGTAAAGGAGAAGGTCC) and #6250 (CCGGCTAGCTTAGTCGACTTCCTCGATCTTGGG) (*XhoI* and *NheI*) respectively. The obtained PCR products were digested with the specific restrictions enzymes and cloned into the pESC-Trp-Cup vector. The plasmids pTRV1 and pTRV2-pPDS for virus-induced gene silencing (VIGS) were kindly provided by S. Dinesh-Kumar (UC Davis). pTRV2-cGFP was used as control (Xu et al., 2014).

To construct the plant pTRV2-NbErd2-3′ plasmid, a 3′ portion of *NbERD2* was PCR-amplified using *N. benthamiana* cDNA with primers #5497 (GCCGGATCCGCATACAACATGAGGAACAC) and #5498 (CGGCTCGAGGATTACAGACGCTCTCCAAC). For VIGS constructs

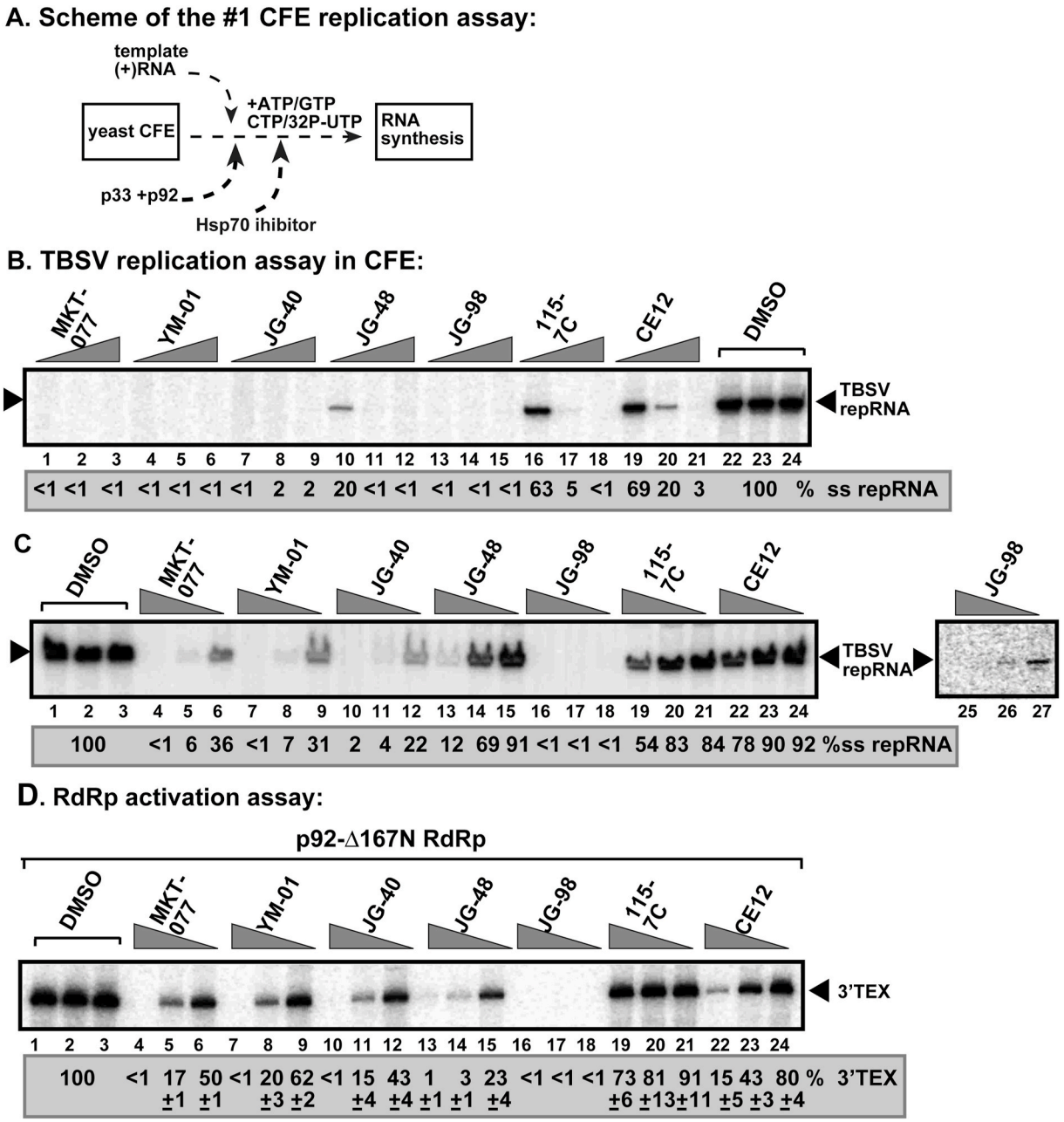

Fig. 9. Inhibition of *in vitro* reconstitution of TBSV replicase by allosteric inhibitors of Hsp70. (A) Scheme of the CFE-based TBSV replicase reconstitution assay in the presence of the small molecule allosteric inhibitors. The yeast CFE was programmed with *in vitro* transcribed TBSV DI-72 (+)repRNA and purified recombinant MBP-p33 and MBP-p92^{pol} replication proteins of TBSV. (B) Denaturing PAGE analysis of the ^{32}P-labeled TBSV repRNA products obtained in the CFE-based TBSV replicase reconstitution assay. repRNA production was measured using ImageQuant software. The final amounts for each compound were 111.1 μM, 333.3 μM, and 1000.0 μM, respectively, in the replicase reconstitution assay, whereas DMSO solvent was present in 10% in each sample. The experiments were repeated two times. (C) Similar PAGE analysis of the ^{32}P-labeled TBSV repRNA products obtained in the CFE-based TBSV replicase reconstitution assay as in panel B, except with lesser amounts of inhibitors. The final amounts for each compound were 111.1 μM; 37.0 μM and 12.3 μM, respectively, in the replicase reconstitution assay, whereas DMSO solvent was present in 10% in each sample. Note that the most effective inhibitor JG-98 was also applied in 12.3 μM (lane 25), 4.1 μM (lane 26) and 1.4 μM (lane 27) in the assay. The experiments were repeated two times. (D) Denaturing PAGE analysis of the ^{32}P-labeled RNA products of DI-72 (+)RNA obtained in an *in vitro* assay with the activated recombinant p92-Δ167N RdRp. The amounts of 3′TEX products were estimated using the ImageQuant software. The experiments were repeated two times.

pTRV2-AtErd2-5′ and pTRV2-AtErd2-3', we PCR-amplified *AtERD2* sequences with primers #6267 (GCCGGATCCATGGCTGGTAAGGGAGAAGGTC) and #6268 (CGGCTCGAGTCTGCTTGTCCAGGGGTTACC) and #6269 (GCCGGATCCGAAGATGGTGCAAGAAGCTGAG) and #6270 (CGGCTCGAGCATCCTTGATACATCTTAGTGATGATGGTAC), respectively. The obtained PCR products were digested with *Bam*HI and *XhoI* and ligated into pTRV2 plasmid digested with *Bam*HI and *XhoI*.

To make the plant expression vectors, pGD-2x35S-L-AtERD2 and pGD-2x35S-L-*At*Hsp70-2, the *AtERD2* gene sequence was PCR-amplified using primers #5643 and #5646 as explained above, digested with *BamH* and *XhoI* and inserted into pGD-2x35S-L vector digested with *Bam*HI and *XhoI*. *AtHSP70-2* gene sequence was PCR-amplified using primers #6300 (CCGCTCGAGATGGCTGGTAAAGGAGAAGGTCC) and #6299 (CCGGAGCTCTTAGTCGACTTCCTCGATCTTGGG). The obtained PCR product was digested with *XhoI* and *SacI* and inserted into the pGD-2x35S-L vector digested with *XhoI* and *SacI*.

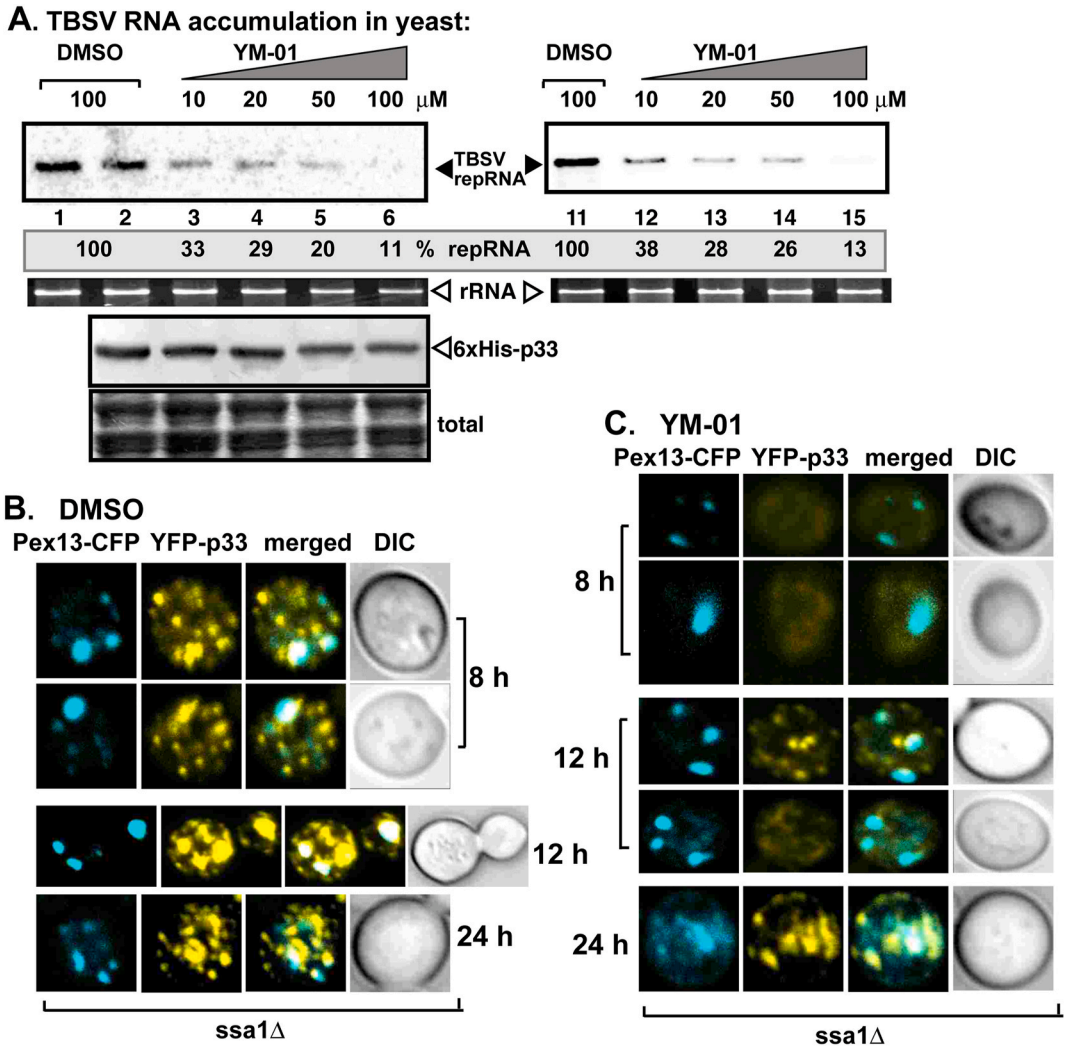

Fig. 10. Inhibition of TBSV repRNA accumulation by YM-01 small chemical allosteric inhibitor of Hsp70 in yeast. (A) Dose-dependent inhibition of TBSV repRNA accumulation in yeast treated with YM-01. Top image: Northern blotting of TBSV repRNA accumulation in yeast treated with YM-01 as shown in two biological replicates. DMSO solvent was present in 10% in each treatment. The yeasts co-expressed the tombusvirus His_6-p33 and His_6-p92 replication proteins and the TBSV DI-72 repRNA from plasmids for 24 h at 23 °C. The accumulation level of repRNA was measured using ImageQuant software. Middle panel: Ribosomal RNA was used as a loading control. Bottom images: Western blotting shows the accumulation levels of His_6-p33 with His_6-p92 in the above yeast samples. Coomassie blue-stained SDS-PAGE shows total protein loading. (B–C) Confocal microscopy images show delayed co-localization of the YFP-p33 replication protein and the Pex13-CFP peroxisomal marker in yeast treated with YM-01 allosteric inhibitor of Hsp70. The p33 replication protein forms large VRO-like structures with aggregated peroxisomes and ER membranes in yeast (ssa1Δ strain) visible as punctate structures in the control yeast even at early time points, whereas YFP-p33 shows diffused localization at early time points and it only forms punctate structures late in YM-01-treated yeast (24 h at 23 °C).

Analysis of Hsp70 protein levels in plants. *N. benthamiana* plants (4 weeks old) were sap-inoculated with TBSV or CIRV and total protein was extracted from the systemically-infected leaves 4 days post-infection (dpi) and 6 dpi, respectively. The total protein of the plants was extracted as follows: 2 discs of plant samples were frozen with liquid nitrogen and ground in 100 μl of 1x SDS-PAGE loading buffer +5 μl β-mercaptoethanol + 25 mM NaCl. The samples were boiled for 15 min and centrifuged at 21,000×*g* for 2 min at RT, and the supernatants were transferred to new Eppendorf tubes and the protein samples were analyzed by sodium dodecyl sulfate-polyacrylamide gel (SDS/10% PAGE). Western blotting was performed using plant anti-Hsp70 monoclonal antibody (5B7 from Enzo) as a first antibody followed by the secondary anti-mouse immunoglobulin G antibody (Sigma) (Wang et al., 2009).

Semi-quantitative RT-PCR analysis of *ERD2* mRNA. *N. benthamiana* plants were sap-inoculated with TBSV or CIRV, followed by total RNA isolation from systemically-infected leaves, 4 and 5 dpi, respectively. Plant RNA samples were treated with DNAse for 1 h at 37 °C, and then, the samples were extracted with phenol-chloroform. The RNA quality was checked with agarose gelelectrophoresis. The RT-PCRs were performed using the oligos: #5497 (GCCGGATCCGCATACAACATGAGGAACAC) and #5498 (CGGCTCGAGGATTACAGACGCTCTCCAAC) based on *N. benthamiana ERD2* RNA sequence and primers #6481 (AAGTGGGGTACATGATGTGGTTC) and #6485 (CCATAGTAGCTCCACCAGCA) based on *Solanum lycopersicum* putative mERD2 sequence. As an internal control, we RT-PCR-amplified Tubulin mRNA with oligos #2859 (TAATACGACTCACTATAGGAACCAAATCATTCATGTTGCTCTC) and #2860 (TAGTGTATGTGATATCCCACCAA).

Real time qRT-PCR of *ERD2* mRNA. *N. benthamiana* plants were inoculated with TBSV or CIRV, total RNA was extracted from the infected leaves 2 dpi and 3 dpi, respectively. For the systemic leaves, samples were collected at 4 dpi for TBSV and 5 dpi for CIRV. Plant RNA was extracted and analyzed in an ethidium bromide gel to adjust the samples loading. To make the cDNA, we used MMLV reverse transcriptase 1st strand cDNA synthesis kit (Lucigen) and Oligo DT. The primers for the Real time RT-PCR assay were designed using Real Time

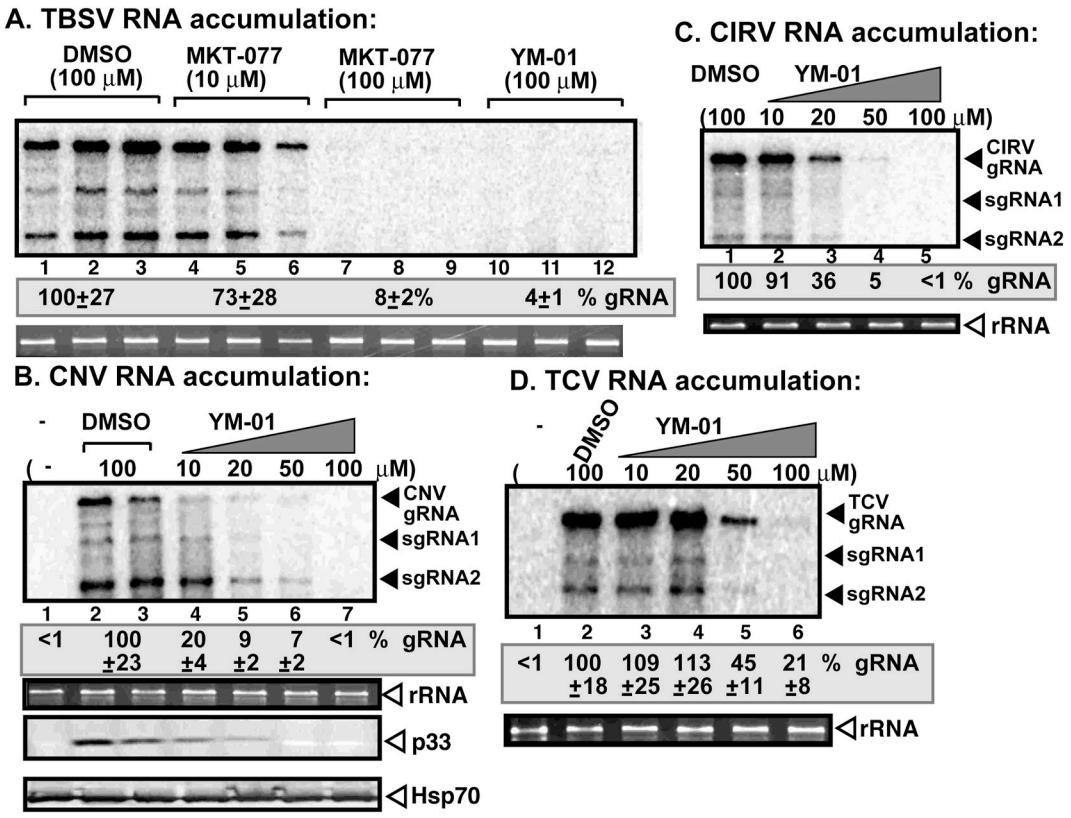

Fig. 11. Inhibition of TBSV genomic RNA accumulation by small chemical allosteric inhibitors of Hsp70 in *N. benthamiana* protoplasts. (A) Top image: Northern blotting of TBSV RNA accumulation in *N. benthamiana* protoplasts (single cells lacking cell-walls) treated with 10 or 100 μM inhibitors as shown. The protoplasts were electroporated with 1 μg TBSV RNA followed by incubation in the presence of the inhibitors for 24 h at 23 °C. DMSO solvent was present in 10% in each treatment. The accumulation level of gRNA was measured using ImageQuant software. Middle panel: Ribosomal RNA was used as a loading control. (B) Tope image: Northern blot shows dose-dependent CNV RNA accumulation in *N. benthamiana* protoplasts treated with the YM-01 allosteric inhibitor. See panel A for additional details. Bottom images: Western blotting shows the accumulation levels of p33 and Hsp70 detected with anti-p33 and anti-Hsp70 antibodies in the above protoplasts samples. (C) Northern blot shows dose-dependent CIRV RNA accumulation in *N. benthamiana* protoplasts treated with YM-01 allosteric inhibitor. See panel A for additional details. (D) Northern blot shows dose-dependent TCV RNA accumulation in *N. benthamiana* protoplasts treated with YM-01 allosteric inhibitor. See panel A for additional details. The experiments were repeated three times and two times in case of CIRV.

qPCR Assay Entry Tool from Integrated DNA Technologies website (https://www.idtdna.com/pages) and *NbERD2* putative gene sequence as a reference. We performed the assay using Applied Biosystem Power up™ SYBR® green master mix (Thermo Fisher Scientific) oligos #8352 (TCCAATGGCTTGACGATAACC) and #8353 (GACACTCTCCAACTCCTTCATC). As an internal control, the *N. benthamiana* housekeeping tubulin gene was RT-PCR-amplified with oligos #8178 (CTGGGAAGTTATCTGTGACGA) and #8179 (AACAGCCCTAGGAACATAACG). The reactions were placed in the Eppendorf® Mastercycle® in a 96 well plate (ABI background plate) and the PCR conditions were selected following the Power up™ SYBR® green master mix manual recommendations. Data was analyzed with Excel program.

Total protein extraction from yeast and Western blot analysis. Yeast total protein was harvested then resuspended in 0.1 M NaOH and vortexing for 30 s, followed by shaking for 15 min. The samples were centrifuged at 21,000×*g* for 1 min and the supernatant was discarded. We then added 1x SDS-PAGE loading buffer + β-mercaptoethanol to the pellet, vortexed the samples for 30 s, shaked for 15 min and the samples were placed at 85 °C for 15 min. Protein samples were analyzed in SDS-10% PAGE gels, followed by electrotransfer to a PVDF membrane (BioRad). The membranes were treated with 5% nonfat dry milk solution in Tris-buffered saline (TBS) buffer containing 0.1% Tween 20 (T-TBS). The membranes were washed three times with T-TBS buffer and incubated with primary antibody overnight at 4 °C. Then, the membranes were washed with T-TBS buffer 3 times for 5 min and incubated with the secondary alkaline phosphatase-conjugated antibody. After washing, the membranes were developed using 5-bromo-4-chloro-3indolylphosphate and nitro-blue tetrazolium (Sigma) in 100 mM Sodium bicarbonate buffer pH 9.5.

Strep-affinity protein purification assay. BY4741 yeast strain was co-transformed with plasmids pESC-StrepC33/DI72, pYES-StrepC92 (Xu et al., 2014) and pRS315-Nflag-AtERD2 or pRS315-Nflag-ssa1 or pRS315-Nflag-*At*Hsp70-2 by the LiAc-single-stranded DNA-polyethylene glycol method (Panavas and Nagy, 2003). As a control, we also co-transformed yeast with plasmids: pESC-HisCNVp33-DI72, pYES-CNVp92 and pRS315-Nflag-AtERD2 or pRS315-Nflag-ssa1 or pRS315-Nflag-AtHsp70-2 (Xu et al., 2014). BY4741 yeast strain co-expressing strep-C33/DI72, strep-C92 and Nflag-AtERD2 or Nflag-ssa1 or Nflag-*At*Hsp70-2 or the control yeast expressing HisCNVp33-DI72, CNVp92, and Nflag-AtERD2 or Nflag-ssa1 or Nflag-AtHsp70-2 were grown in 15 ml SC–ULH$^-$ (Ura-/Leu-/His-) media supplemented with 2% glucose for 24 h. Then, the yeast cultures were washed and inoculated in 50 ml SC–ULH$^-$ media supplemented with 2% galactose, followed by culturing for 24 h at 23 °C. The pellets were washed with 50 mM Tris-HCl pH7.5 and harvested by centrifugation 21,000×*g* for 5 min. Two hundred milligrams of the yeast pellets were broken in 200 μl of Yeast Lysis Buffer (50 mM Tris-HCl, pH7.5; 15 mM $MgCl_2$, 10 mM KCl, 10 mM β-mercaptoethanol, Yeast Protease Inhibitor Mix [Sigma]). The extracts were centrifuged at 1000×*g* for 10 min, and the supernatants were transferred to a new Eppendorf tube, followed by centrifugation at 21,000×*g* for 30 min at 4 °C. The supernatants were discarded. The membrane fraction of the yeast pellets was solubilized in

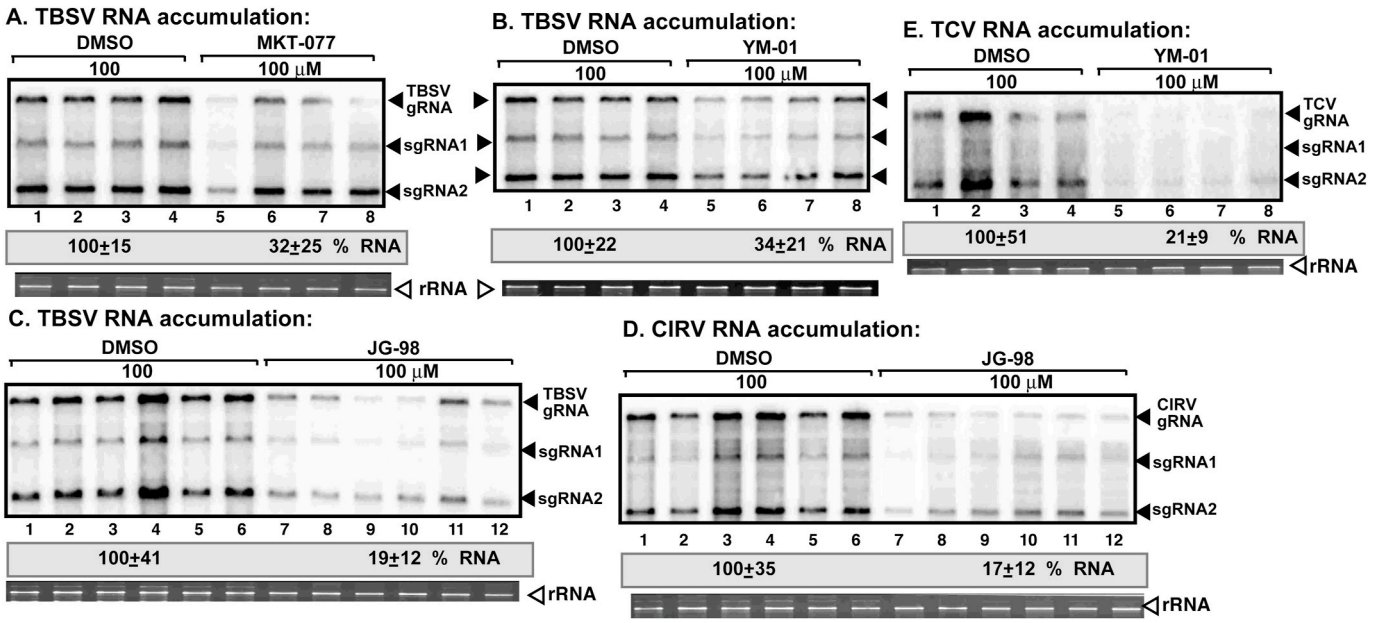

Fig. 12. Inhibition of TBSV and related viruses by chemical allosteric inhibitors of Hsp70 in *N. benthamiana* plants. (A–C) Top image: Northern blotting of TBSV RNA accumulation in *N. benthamiana* leaves infiltrated 1 h and repeatedly at 6 h after sap-inoculation with 100 μM inhibitors as shown. DMSO solvent was present in 10% in each treatment. The total RNA was isolated after 17 h incubation at 23 °C. The accumulation level of gRNA was measured using ImageQuant software. Bottom panel: Ribosomal RNA was used as a loading control. (D) Comparable experiments on CIRV RNA accumulation in *N. benthamiana* treated with the JG-98 allosteric inhibitor. See panel A for additional details. (E) Comparable experiments on TCV RNA accumulation in *N. benthamiana* treated with the YM-01 allosteric inhibitor. See panel A for additional details. The experiments were repeated three times.

the Solubilization Buffer and gently rotated at 4 °C for 4 h. To prepare the samples for the Strep-affinity purification, the solubilized membrane fractions were centrifuged at 21,000×*g* for 20 min at 4 °C and the supernatants suspension (IBA Life Sciences). Then, the samples were applied to columns. each containing 25 μl of StrepTactin Superflow high capacity. The columns were rotated for 4 h, followed by washing with two volumes of the column buffer and two volumes of washing buffer. We added 40 μl SDS-PAGE sample buffer directly to resin in the columns and incubated the columns for 15 min at 85 °C in Eppendorf tubes. The samples were collected via centrifugation of the columns at 600×*g* for 5 min at RT. 2 μl of β-mercaptoethanol was added to the samples, followed by incubation at 85 °C for 15 min. The affinity-purified Strep-p33/-Strep-p92 samples were tested for the presence of Flag-AtErd2, Flag-ssa1 or Flag-*At*Hsp70-2 using 10% SDS-PAGE. Western Blot was performed using anti-Strep-tag antibody (2 μl in 10 ml 5%T-TBS Milk), anti-Flag antibody (1 μl in 10 ml 5%T-TBS Milk) and anti-His antibody (1 μl in 10 ml 5%T-TBS Milk) as the primary antibodies. After through washing of the membranes, secondary alkaline phosphatase-conjugated antibody anti-mouse immunoglobulin (Sigma) (Xu et al., 2014) was applied to the membranes to detect the co-purified proteins.

Complementation experiments in double yeast mutant *ssa1 ssa2*. Double mutant *ssa1 ssa2* yeast strain was co-transformed with the TBSV expression plasmids (pRS317-TET-His92, pURA-His33/DI72) or the CIRV expression plasmids (pRS317-TET-flag95, pESC(U)-His36/DI72) (Barajas et al., 2014). The yeasts were also transformed with one of the following plasmids: pESC-Trp-Cup-ssa1, pESC-Trp-Cup-AtERD2 or pESC-Trp-Cup-AtHsp70-2 (Panavas and Nagy, 2003). Yeasts were plated onto SC–UKLHT$^-$ (Ura-/Lys-/Leu-/His-/Trp-) media and grown at 23 °C for 6 d. Transformed yeasts were grown for 24 h at 23 °C in SC–KUT$^-$ (-Lys/Ura-/Trp) media supplemented with 2% glucose, following by replacing the media SC–KUT$^-$ media supplemented with 2% galactose and 50 μM $CuSO_4$ at 23 °C for 24 h for AtHsp70-2 and for 36 h for yeast expressing AtErd2. The cells were harvested to extract RNA and protein. The protein levels of p33, p92, p36 replication proteins were detected with Western blot using anti-His antibody, while p95, ssa1, AtErd2, AtHsp70-2 were detected using anti-Flag antibody, followed by secondary anti-mouse immunoglobulin.

Northern blot analysis. Yeast total RNA was extracted with Extraction Buffer (50 mM sodium acetate [pH 5.2], 10 mM EDTA, 1% SDS) and water-saturated phenol. Samples were vortexed and incubated for 4 min at 65 °C and centrifuged at 21,000×*g* for 15 min at 4 °C. Total RNA was precipitated from the aqueous phase by adding 3 vol of absolute ethanol with 30 mM of Sodium Acetate and the pellet was washed with 70% ethanol. Total RNA was dissolved in RNase-free water, followed by heat-treatment (5 min at 85 °C), and 1.5% agarose gel electrophoresis. The total RNA was transferred to Hybond XL membrane (Amersham) and cross-linked with UV (Bio-Rad). RNA hybridization was done in ULTRAhyb solution (Ambion) at 68 °C according to the supplier's instructions. The ^{32}P-UTP-labeled DI-72 (representing the minus-strand RIII/IV sequence) was used as probes for hybridization. RNA probe signals were detected using a Typhoon 9400 imaging scanner (Amersham) and quantified by ImageQuant software.

The P^{32} –labeled radioactive probes were done using T7 RNA polymerase (Thermo Fisher Scientific) and the PCR products of a genomic region of TBSV and CNV with primers #1166 (ATTCCTGTTTACGAAAGTTAGGT) and #22 (GTAATACGACTCACTATAGGGCTGCATTTCTGCAATGTTCC), and for CIRV with primer pairs #978 (TAATACGACTCACTATAGGGCTGCATTTCTGCAATGTTC) and #979 (GGACGGAAGCTTCACTGCACAGAGT), for RCNMV with primer pairs #3043 (AGGGGAACACGCAGTCTC) and #3044 (TAATACGACTCACTATAGGATTTTGTTTTACCAGAGGTATGC). The P^{32}-labeled TBSV, CIRV, CNV and RCNMV minus-stranded probes were purified using a Micro Bio-Spin column P-30® (Bio-Rad) and used as probes for hybridization. Hybridization signals were detected using a Typhoon 9400 imaging scanner (Amersham) and quantified by Image Quant software (Panaviene et al., 2004a).

Knock down of Hsp70s in *N. benthamiana*. Virus-induced gene silencing (VIGS) in *N. benthamiana* was done as previously described (Jaag and Nagy, 2009). Briefly, *Agrobacterium tumefaciens* strain C58C1 carrying pTRV1 (OD_{600} 0.05) (a gift from Dinesh-Kumar, UC Davis) in combination of one of the plasmids: pTRV2-NbERD2-3' (OD_{600} 0.05), pTRV2-*At*ERD2-5' (OD_{600} 0.05) or pTRV2-*At*ERD2-Cterm (OD_{600} 0.05)

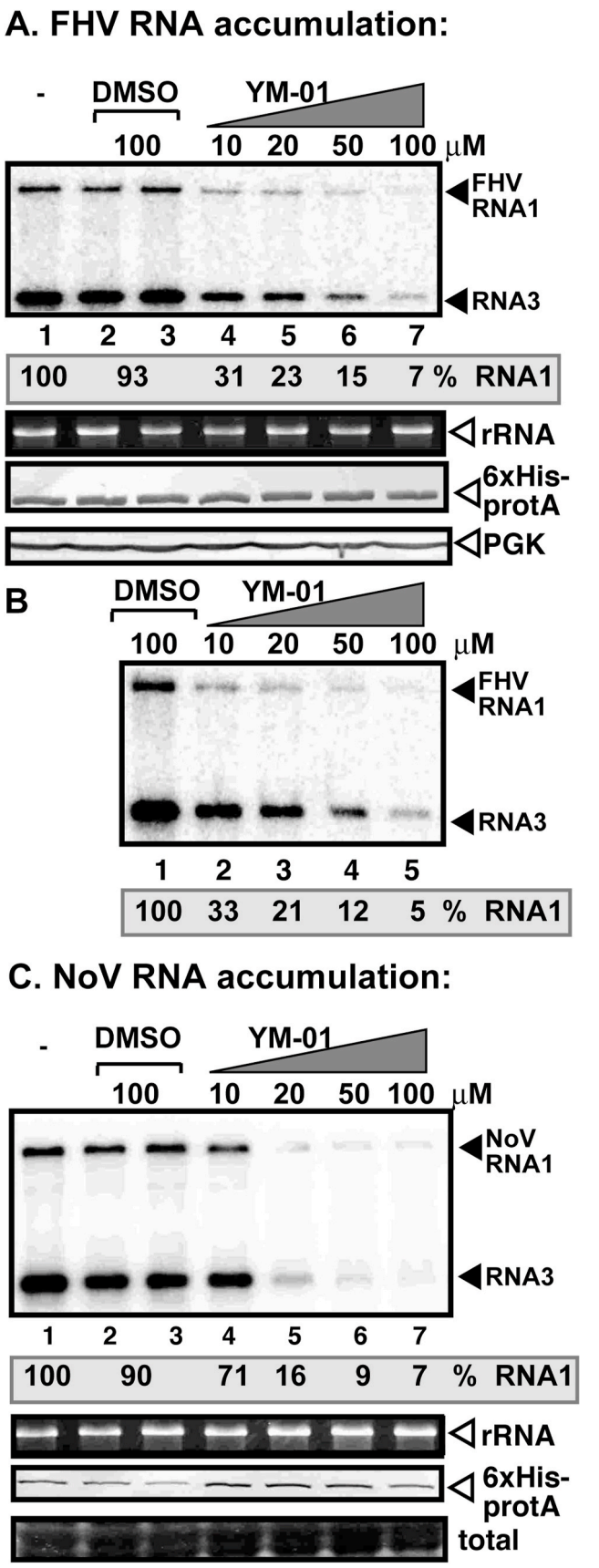

(caption on next column)

Fig. 13. Inhibition of nodavirus accumulation by YM-01 allosteric inhibitor of Hsp70 in yeast. (A–B) Top image: Northern blot analysis of FHV RNA1 and the subgenomic RNA3 accumulation in yeast treated with YM-01 allosteric inhibitors as shown in two biological replicates. The yeasts co-expressed the FHV His_6-protein A RdRp and RNA1 from plasmids for 24 h at 23 °C. DMSO solvent was present in 10% in each treatment. The accumulation level of RNA1 was measured using ImageQuant software. Middle panel: Ribosomal RNA was used as a loading control. Bottom images: Western blotting shows the accumulation levels of His_6-protein A RdRp in the above yeast samples. The yeast Pgk1 was detected by anti-Pgk1 antibody using western blotting. (C) Dose-dependent inhibition of NoV RNA1 and sgRNA3 accumulation in yeast treated with YM-01 inhibitor. See further details in panel A above. The experiments were repeated two times.

were infiltrated into leaves of *N. benthamiana* (Jaag and Nagy, 2009). Seven days post agroinfiltration, the upper leaves were sap-inoculated with $CNV^{20KStop}$ (not expressing the p20 silencing suppressor), TBSV, CIRV or RCNMV. For the analysis of viral RNA accumulation, total RNA was extracted 2.5 d for $CNV^{20KStop}$, 2 d for TBSV, and 3 d for CIRV samples after inoculation from the infected leaves and 6 dpi in case of RCNMV. The ^{32}P-labeled TBSV, CIRV, CNV and RCNMV probes were used for RNA hybridization. Hybridization signals were detected using a Typhoon 9400 imaging scanner (Amersham) and quantified by Image Quant software (Panaviene et al., 2004a). The knockdown level of NbERD2 mRNA was checked at the 7th day post agroinfiltration by semi-quantitative RT-PCR using primers #5494 (GCCGGATCCCTCG-GAACCACGTATTCCTG) and #5495 (CGGCTCGAGGTAGGCTCATTGA-TAATACG). Total plant protein was extracted and Hsp70's levels were detected with western blotting using plant anti-Hsp70 monoclonal antibody as described above.

Overexpression of plant proteins in *N. benthamiana*. *A. tumefaciens* strain C58C1 carrying one of the following constructs: pGD-2x35S-L-*At*ERD2 (OD_{600} 0.6), pGD-2x35S-L-*At*Hsp70-2 (OD_{600} 0.6) or pGD-2x35S-L (OD_{600} 0.6), were co-agroinfiltrated with pGD-p19 (OD_{600} 0.2) and pGD-35S–$CNV^{20Kstop}$ (OD_{600} 0.2) into young *N. benthamiana* leaves as before (Barajas et al., 2009). Total RNA was extracted from agroinfiltrated leaves 2 ½ days after agroinfiltration, followed by northern blotting as described above.

Confocal laser microscopy in plants. For the bimolecular fluorescence complementation (BiFC) assay, agrobacterium carrying plasmids pGD-cYFP-T33 and pGD-nYFP-AtErd2 or pGD-nYFP-AtHsp70-2 and RFP-SKL were co-agroinfiltrated into the *N. benthamiana* leaves. For the TBSV infected sample, the agroinfiltrated leaves were inoculated with TBSV sap 24 h after agroinfiltration and the plant samples were visualized 50 h after agroinfiltration. For the CIRV experiments, plant leaves were co-infiltrated with agrobacteria carrying pGD-cYFP-C36 and pGD-nYFP-AtErd2 or pGD-nYFP-AtHsp70-2 and RFP-Tim21, as the mitochondrial marker. For the CIRV infected leaves, the agrobacterium carrying pGD-CIRV was co-infiltrated with the BiFC plasmids mentioned above. 50 h after agroinfiltration the plant samples were analyzed using confocal laser microscopy. As a control, plants were co-agroinfiltrated with agrobacteria carrying pGD-cYFP and pGD-nYFP-AtErd2 or pGD-nYFP-Hsp70- 2. To observe the subcellular distribution of Erd2 and Hsp70-2 in *N. benthamiana*, plant leaves were co-infiltrated with agrobacteria transformed with pGD-BFP-T33, pGD-RFP-SKL, pGD-EGFP-AtErd2 or pGD-EGFP-AtHsp70-2. Agroinfiltrated leaves were inoculated with TBSV sap 24 h after agroinfiltration. For CIRV, plant leaves were co-agroinfiltrated with pGD-BFP-C36, pGD-CIRV, pGD-EGFP-AtEtd2 or pGD-EGFP-AtHsp70-2 and pGD-RFP-Tim21. Plant samples were analyzed 50 h after agroinfiltration with confocal laser microscopy.

Purification of Flag-tagged proteins from yeast. The recombinant Flag-*At*Erd2, Flag-*At*Hsp70-2, Flag-ssa1 proteins were expressed from pESC-Trp-Cup-AtERD2, pESC-Trp-Cup-AtHsp70-2, pESC-Trp-Cup-ssa1 in Sc1 yeast strain (Barajas et al., 2009). Sc1 strain expressing one of the recombinant proteins was grown at 23 °C in SC^{Trp-} supplemented

with 2% glucose for 24 h, then the OD_{600} of the yeast cultures was adjusted to 0.4, followed by dilution in 100 ml of minimal media SC^{Trp-} supplemented with 2% glucose and 50 μM of $CuSO_4$. Yeasts were further cultured for 6 h at 23 °C. Yeast cells (200 mg) were broken in 200 μl of yeast breaking buffer (1 M HEPES-KOH pH7.6, 1 M Potassium Acetate sterile, 1 M Magnesium Acetate sterile, β-mercaptoethanol, protease inhibitor mix [Sigma]), followed by centrifugation at 400×*g* for 3 min at 4 °C. The supernatants were pipetted to a fresh tube, centrifuged at 21,000×*g* for 15 min at 4 °C and transferred to an equilibrated Flag-column and rotated at 4 °C for 2 h. The columns were centrifuged at 100×*g* for 2 min at 4 °C and washed three times with the Washing Buffer (1 M HEPES-KOH pH7.6, 1 M Potassium Acetate sterile, 1 M Magnesium Acetate sterile). The recombinant proteins were eluted from the column with the Flag elution buffer (1 M HEPES-KOH pH7.6, 1 M Potassium Acetate sterile, 1 M Magnesium Acetate sterile, 2 μl Flag peptide) after incubation on ice for 3 h. The Flag-tagged proteins were collected by centrifugation at 100×*g* for 2 min at 4 °C and stored at −80 °C for further experiments.

Protoplasts isolation and Hsp70 allosteric inhibitors treatment. Protoplasts were isolated form N. *benthamiana* callus as previously described (Panaviene et al., 2003). Newly prepared protoplasts were treated with 100 μM of DMSO or different concentrations (10, 20, 50 & 100 μM) of Hsp70 allosteric inhibitors for 30 min, followed by electroporation with 1 μg of *in vitro* transcribed TBSV, CNV and TCV gRNAs, respectively. After electroporation, samples were kept on ice for 30 min, followed by addition of 0.7 ml of protoplast culture medium to each sample. Protoplasts were transferred to 35 × 10 mm petri dishes and incubated in dark for 24 h at room temperature, followed by RNA analysis (Panaviene et al., 2003).

Hsp70 allosteric inhibitors treatment in plants. *N. benthamiana* leaves were first infiltrated with 50 μM DMSO or Hsp70 inhibitors. After 1 h incubation, the same leaves were sap-infected with TBSV, CNV or TCV. 6 h later, the same leaves were infiltrated with 100 μM DMSO or Hsp70 inhibitor (MKT-077 or YM-01), after 17 h total RNA was isolated from the infected leaves.

Treating yeast with Hsp70 allosteric inhibitors. The yeast strain BY4741 was co-transformed with HpGBK-CUP1-p33/Gal-DI-72 and LpESC-CUP1-His-p92 as described (Panavas and Nagy, 2003). Transformed yeast cells were inoculated in LH^- media supplemented with 2% glucose and BCS at 23 °C for 12 h. Then, the media with LH^- media (inhibitor uptake media contained 0.003%SDS) supplemented with 2% galactose and 50 μM $CuSO_4$ in presence of 100 μM DMSO or 10, 20, 50 & 100 μM of inhibitors. Yeasts were grown at 23 °C for 24 h. Then, total RNA was isolated and analyzed as described earlier (Cheng et al., 2005; Panaviene et al., 2004b).

***In vitro* TBSV RdRp activation assay.** The recombinant MBP-p92-Δ167N TBSV RdRp (Pogany and Nagy, 2012) was purified from *E. coli*. Briefly, bacteria culture was grown in MB broth supplemented with 100 μg/ml ampicillin and 34 μg/ml chloramphenicol at 37 °C until reaching OD_{600} 0.7. The recombinant protein expression was induced with 1 mM IPTG for 8 h at 16 °C, followed by sonication in cold Column Buffer with reduced salt containing β-mercaptoethanol. Then, the samples were centrifuged 21,000×*g* and the supernatant was transferred into a column containing 0.4 ml amylose resin. The columns were rotated for 30 min, washed 5 times with cold Column Buffer with reduced salt, followed by elution of the purified proteins in 0.3 ml MBP Elution Buffer and stored at −80 °C (Pogany and Nagy, 2012). The full-length TBSV DI-72 (+)RNA and DI-72-mini (+)RNA transcripts were prepared as before (Pogany and Nagy, 2015). The Flag-affinity purified host proteins from yeast or the yeast soluble fraction (as a control) were incubated together with the recombinant MBP-p92-Δ167N in a buffer containing 50 mM potassium acetate, 5 mM magnesium acetate, 0.2 M sorbitol, 0.2 μl actinomycin D (5 mg/ml), 0.2 μl 1 M DTT, 2 μl of 150 mM creatine phosphate, 2 μl of 10 mM ATP, CTP, and GTP and 0.25 mM UTP, 0.1 μl of [^{32}P]UTP, 0.2 μl of 10 mg/ml creatine kinase, 0.2 μl of RNase inhibitor, 2 μl DMSO, and 0.5 μg (+)RNA transcript in a 20 μl reaction mixture (Pogany and Nagy, 2015). The final reaction was incubated at 25 °C for 3 h, then the reactions were stopped with the SDS stop solution (1% SDS, 0.05 M EDTA pH8.0), followed by RNA precipitation with isopropanol-1 M Ammonium Acetate and washed with 70% ethanol. The RNA samples were dissolved in 1X RNA loading dye and analyzed in a 5% Acrylamide/8 M urea gel (Pogany and Nagy, 2015).

***In vitro* reconstitution of the TBSV replicase in yeast membrane fraction.** To reconstitute the TBSV replicase, yeast cell-free extract (CFE) was prepared from BY4741 strain as described previously (Pogany and Nagy, 2008). The CFE membrane fraction was obtained by centrifugation of the CFE as before (Kovalev et al., 2014). MBP-p92 and MBP-p33 recombinant proteins were purified as described above (Pogany and Nagy, 2012). For the reconstitution assay, the CFE membrane fraction was incubated with the recombinant MBP-p92 and MBP-p33 proteins and one of the following purified recombinant proteins: Flag-Ssa1, Flag-AtErd2 or Flag-Hsp70-2 in a buffer containing 50 mM potassium acetate, 5 mM magnesium acetate, 0.2 M sorbitol, 0.2 μl actinomycin D (5 mg/ml), 2 μl of 150 mM creatine phosphate, 2 μl of 10 mM ATP, CTP, and GTP and 0.25 mM UTP, 0.1 μl of [^{32}P]UTP, 0.2 μl of 10 mg/ml creatine kinase, 0.2 μl of RNase inhibitor, 0.2 μl of 1 M DTT, and 0.5 μg DI-72 (+)RNA transcripts in a 20 μl reaction mixture (Pogany and Nagy, 2008). The final reaction was incubated at 25 °C for 3h followed by addition of SDS stop solution, and RNA precipitation with isopropanol Ammonium Acetate. The *in vitro* replicase products were analyzed in a 5% Acrylamide/8 M urea gel (Li et al., 2010).

Declaration of interests

The authors declare that they have no known competing financial interests or personal relationships that could have appeared to influence the work reported in this paper.

CRediT authorship contribution statement

Melissa Molho: Conceptualization, Methodology, Validation, Formal analysis, Investigation, Resources, Data curation, Writing, Writing – original draft, Visualization. **K. Reddisiva Prasanth:** Conceptualization, Methodology, Validation, Formal analysis, Investigation, Resources, Data curation, Writing, Writing – original draft, Visualization. **Judit Pogany:** Conceptualization, Methodology, Validation, Formal analysis, Investigation, Resources, Data curation, Writing, Writing – original draft, Visualization. **Peter D. Nagy:** Conceptualization, Validation, Formal analysis, Resources, Data curation, Writing, Writing – original draft, Writing – review & editing, Visualization, Supervision, Project administration, Funding acquisition.

Acknowledgements

The authors thank to Jason E. Gestwicki (Department of Pharmaceutical Chemistry and the Institute for Neurodegenerative Disease, University of California at San Francisco, San Francisco, California) for providing the Hsp70 allosteric inhibitors. This work was supported by the National Science Foundation (MCB-1517751 and IOS-1922895), USDA (NIFA, 2020-70410-32901) and a USDA hatch grant (KY012042) to PDN.

References

Acosta, E.G., Kumar, A., Bartenschlager, R., 2014. Revisiting dengue virus-host cell interaction: new insights into molecular and cellular virology. Adv. Virus Res. 88, 1–109.

Alam, S.B., Rochon, D., 2015. Cucumber necrosis virus recruits cellular heat shock protein 70 homologs at several stages of infection. J. Virol. 90 (7), 3302–3317.

Alam, S.B., Rochon, D., 2017. Evidence that Hsc70 is associated with cucumber necrosis virus particles and plays a role in particle disassembly. J. Virol. 91 (2).

Altan-Bonnet, N., 2017. Lipid tales of viral replication and transmission. Trends Cell Biol. 27 (3), 201–213.

Assimon, V.A., Gillies, A.T., Rauch, J.N., Gestwicki, J.E., 2013. Hsp70 protein complexes as drug targets. Curr. Pharmaceut. Des. 19 (3), 404–417.
Barajas, D., Jiang, Y., Nagy, P.D., 2009a. A unique role for the host ESCRT proteins in replication of tomato bushy stunt virus. PLoS Pathog. 5 (12), 13.
Barajas, D., Li, Z., Nagy, P.D., 2009b. The Nedd4-type Rsp5p ubiquitin ligase inhibits tombusvirus replication by regulating degradation of the p92 replication protein and decreasing the activity of the tombusvirus replicase. J. Virol. 83 (22), 11751–11764.
Barajas, D., Xu, K., Martin, I.F.D., Sasvari, Z., Brandizzi, F., Risco, C., Nagy, P.D., 2014. Co-opted oxysterol-binding ORP and VAP proteins channel sterols to RNA virus replication sites via membrane contact sites. PLoS Pathog. 10 (10).
Becker, J., Walter, W., Yan, W., Craig, E.A., 1996. Functional interaction of cytosolic hsp70 and a DnaJ-related protein, Ydj1p, in protein translocation in vivo. Mol. Cell Biol. 16 (8), 4378–4386.
Bozzacco, L., Yi, Z., Andreo, U., Conklin, C.R., Li, M.M., Rice, C.M., MacDonald, M.R., 2016. Chaperone-assisted protein folding is critical for yellow fever virus NS3/4A cleavage and replication. J. Virol. 90 (6), 3212–3228.
Cao, M., Wei, C., Zhao, L., Wang, J., Jia, Q., Wang, X., Jin, Q., Deng, T., 2014. DnaJA1/Hsp40 is co-opted by influenza A virus to enhance its viral RNA polymerase activity. J. Virol. 88 (24), 14078–14089.
Cazale, A.C., Clement, M., Chiarenza, S., Roncato, M.A., Pochon, N., Creff, A., Marin, E., Leonhardt, N., Noel, L.D., 2009. Altered expression of cytosolic/nuclear HSC70-1 molecular chaperone affects development and abiotic stress tolerance in Arabidopsis thaliana. J. Exp. Bot. 60 (9), 2653–2664.
Cesa, L.C., Patury, S., Komiyama, T., Ahmad, A., Zuiderweg, E.R., Gestwicki, J.E., 2013. Inhibitors of difficult protein-protein interactions identified by high-throughput screening of multiprotein complexes. ACS Chem. Biol. 8 (9), 1988–1997.
Chafekar, S.M., Wisen, S., Thompson, A.D., Echeverria, A., Walter, G.M., Evans, C.G., Makley, L.N., Gestwicki, J.E., Duennwald, M.L., 2012. Pharmacological tuning of heat shock protein 70 modulates polyglutamine toxicity and aggregation. ACS Chem. Biol. 7 (9), 1556–1564.
Cheng, C.P., Panavas, T., Luo, G., Nagy, P.D., 2005. Heterologous RNA replication enhancer stimulates in vitro RNA synthesis and template-switching by the carmovirus, but not by the tombusvirus, RNA-dependent RNA polymerase: implication for modular evolution of RNA viruses. Virology 341 (1), 107–121.
Chenon, M., Camborde, L., Cheminant, S., Jupin, I., 2012. A viral deubiquitylating enzyme targets viral RNA-dependent RNA polymerase and affects viral infectivity. EMBO J. 31 (3), 741–753.
Clerico, E.M., Tilitsky, J.M., Meng, W., Gierasch, L.M., 2015. How hsp70 molecular machines interact with their substrates to mediate diverse physiological functions. J. Mol. Biol. 427 (7), 1575–1588.
de Castro, I.F., Volonte, L., Risco, C., 2013. Virus factories: biogenesis and structural design. Cell Microbiol. 15 (1), 24–34.
de Wilde, A.H., Snijder, E.J., Kikkert, M., van Hemert, M.J., 2018. Host factors in coronavirus replication. Curr. Top. Microbiol. Immunol. 419, 1–42.
Diamond, M.S., Schoggins, J.W., 2013. Host restriction factor screening: let the virus do the work. Cell Host Microbe 14 (3), 229–231.
Duncan, E.J., Cheetham, M.E., Chapple, J.P., van der Spuy, J., 2015. The role of HSP70 and its co-chaperones in protein misfolding, aggregation and disease. Subcell. Biochem. 78, 243–273.
Evans, C.G., Chang, L., Gestwicki, J.E., 2010. Heat shock protein 70 (hsp70) as an emerging drug target. J. Med. Chem. 53 (12), 4585–4602.
Feng, Z., Xu, K., Kovalev, N., Nagy, P.D., 2019. Recruitment of Vps34 PI3K and enrichment of PI3P phosphoinositide in the viral replication compartment is crucial for replication of a positive-strand RNA virus. PLoS Pathog. 15 (1), e1007530.
Fernandez de Castro, I., Fernandez, J.J., Barajas, D., Nagy, P.D., Risco, C., 2017. Three-dimensional imaging of the intracellular assembly of a functional viral RNA replicase complex. J. Cell Sci. 130 (1), 260–268.
Ferradini, N., Iannacone, R., Capomaccio, S., Metelli, A., Armentano, N., Semeraro, L., Cellini, F., Veronesi, F., Rosellini, D., 2015. Assessment of heat shock protein 70 induction by heat in alfalfa varieties and constitutive overexpression in transgenic plants. PloS One 10 (5), e0126051.
Gancarz, B.L., Hao, L., He, Q., Newton, M.A., Ahlquist, P., 2011. Systematic identification of novel, essential host genes affecting bromovirus RNA replication. PloS One 6 (8), e23988.
Gestwicki, J.E., Shao, H., 2019. Inhibitors and chemical probes for molecular chaperone networks. J. Biol. Chem. 294 (6), 2151–2161.
Huang, T.S., Nagy, P.D., 2011. Direct inhibition of tombusvirus plus-strand RNA synthesis by a dominant negative mutant of a host metabolic enzyme, glyceraldehyde-3-phosphate dehydrogenase, in yeast and plants. J. Virol. 85 (17), 9090–9102.
Huang, Y.W., Hu, C.C., Lin, N.S., Hsu, Y.H., 2012. Unusual roles of host metabolic enzymes and housekeeping proteins in plant virus replication. Curr Opin Virol 2 (6), 676–682.
Hyodo, K., Okuno, T., 2020. Hijacking of host cellular components as proviral factors by plant-infecting viruses. Adv. Virus Res. 107, 37–86.
Imura, Y., Molho, M., Chuang, C., Nagy, P.D., 2015. Cellular Ubc2/Rad6 E2 ubiquitin-conjugating enzyme facilitates tombusvirus replication in yeast and plants. Virology 484, 265–275.
Jaag, H.M., Nagy, P.D., 2009. Silencing of Nicotiana benthamiana Xrn4p exoribonuclease promotes tombusvirus RNA accumulation and recombination. Virology 386 (2), 344–352.
Jiang, Y., Serviene, E., Gal, J., Panavas, T., Nagy, P.D., 2006. Identification of essential host factors affecting tombusvirus RNA replication based on the yeast Tet promoters Hughes Collection. J. Virol. 80 (15), 7394–7404.
Khachatoorian, R., Riahi, R., Ganapathy, E., Shao, H., Wheatley, N.M., Sundberg, C., Jung, C.-L., Ruchala, P., Dasgupta, A., Arumugaswami, V., 2016. Allosteric heat shock protein 70 inhibitors block hepatitis C virus assembly. Int. J. Antimicrob. Agents 47 (4), 289–296.
Kiyosue, T., Yamaguchi-Shinozaki, K., Shinozaki, K., 1994. Cloning of cDNAs for genes that are early-responsive to dehydration stress (ERDs) in Arabidopsis thaliana L.: identification of three ERDs as HSP cognate genes. Plant Mol. Biol. 25 (5), 791–798.
Kovalev, N., Pogany, J., Nagy, P.D., 2014. Template role of double-stranded RNA in tombusvirus replication. J. Virol. 88 (10), 5638–5651.
Kovalev, N., Pogany, J., Nagy, P.D., 2020. Reconstitution of an RNA virus replicase in artificial giant unilamellar vesicles supports full replication and provides protection for the dsRNA replication intermediate. J. Virol.
Krishnan, M.N., Ng, A., Sukumaran, B., Gilfoy, F.D., Uchil, P.D., Sultana, H., Brass, A.L., Adametz, R., Tsui, M., Qian, F., Montgomery, R.R., Lev, S., Mason, P.W., Koski, R.A., Elledge, S.J., Xavier, R.J., Agaisse, H., Fikrig, E., 2008. RNA interference screen for human genes associated with West Nile virus infection. Nature 455 (7210), 242–245.
Kushner, D.B., Lindenbach, B.D., Grdzelishvili, V.Z., Noueiry, A.O., Paul, S.M., Ahlquist, P., 2003. Systematic, genome-wide identification of host genes affecting replication of a positive-strand RNA virus. Proc. Natl. Acad. Sci. U. S. A. 100 (26), 15764–15769.
Lamm, C.E., Kraner, M.E., Hofmann, J., Bornke, F., Mock, H.P., Sonnewald, U., 2017. Hop/Sti1 - a two-faced cochaperone involved in pattern recognition receptor maturation and viral infection. Front. Plant Sci. 8, 1754.
Li, Q., Brass, A.L., Ng, A., Hu, Z., Xavier, R.J., Liang, T.J., Elledge, S.J., 2009a. A genome-wide genetic screen for host factors required for hepatitis C virus propagation. Proc. Natl. Acad. Sci. U. S. A. 106 (38), 16410–16415.
Li, X., Colvin, T., Rauch, J.N., Acosta-Alvear, D., Kampmann, M., Dunyak, B., Hann, B., Aftab, B.T., Murnane, M., Cho, M., Walter, P., Weissman, J.S., Sherman, M.Y., Gestwicki, J.E., 2015. Validation of the Hsp70-Bag3 protein-protein interaction as a potential therapeutic target in cancer. Mol. Canc. Therapeut. 14 (3), 642–648.
Li, Z., Barajas, D., Panavas, T., Herbst, D.A., Nagy, P.D., 2008. Cdc34p ubiquitin-conjugating enzyme is a component of the tombusvirus replicase complex and ubiquitinates p33 replication protein. J. Virol. 82 (14), 6911–6926.
Li, Z., Pogany, J., Panavas, T., Xu, K., Esposito, A.M., Kinzy, T.G., Nagy, P.D., 2009b. Translation elongation factor 1A is a component of the tombusvirus replicase complex and affects the stability of the p33 replication co-factor. Virology 385 (1), 245–260.
Li, Z., Pogany, J., Tupman, S., Esposito, A.M., Kinzy, T.G., Nagy, P.D., 2010. Translation elongation factor 1A facilitates the assembly of the tombusvirus replicase and stimulates minus-strand synthesis. PLoS Pathog. 6 (11), e1001175.
Lin, B.L., Wang, J.S., Liu, H.C., Chen, R.W., Meyer, Y., Barakat, A., Delseny, M., 2001. Genomic analysis of the Hsp70 superfamily in Arabidopsis thaliana. Cell Stress Chaperones 6 (3), 201–208.
Lohmus, A., Hafren, A., Makinen, K., 2017. Coat protein regulation by CK2, CPIP, HSP70, and CHIP is required for potato virus A replication and coat protein accumulation. J. Virol. 91 (3).
Manzoor, R., Kuroda, K., Yoshida, R., Tsuda, Y., Fujikura, D., Miyamoto, H., Kajihara, M., Kida, H., Takada, A., 2014. Heat shock protein 70 modulates influenza A virus polymerase activity. J. Biol. Chem. 289 (11), 7599–7614.
Molho, M., Chuang, C., Nagy, P.D., 2021. Co-opting of nonATP-generating glycolytic enzymes for TBSV replication. Virology 559, 15–29.
Moran Luengo, T., Mayer, M.P., Rudiger, S.G.D., 2019. The hsp70-hsp90 chaperone cascade in protein folding. Trends Cell Biol. 29 (2), 164–177.
Nagy, P.D., 2016. Tombusvirus-host interactions: Co-opted evolutionarily conserved host factors take center court. Annu Rev Virol 3 (1), 491–515.
Nagy, P.D., 2017. Exploitation of a surrogate host, Saccharomyces cerevisiae, to identify cellular targets and develop novel antiviral approaches. Curr Opin Virol 26, 132–140.
Nagy, P.D., 2020. Host protein chaperones, RNA helicases and the ubiquitin network highlight the arms race for resources between tombusviruses and their hosts. Adv. Virus Res. 107, 133–158.
Nagy, P.D., Barajas, D., Pogany, J., 2012. Host factors with regulatory roles in tombusvirus replication. Curr Opin Virol 2 (6), 685–692.
Nagy, P.D., Pogany, J., 2012. The dependence of viral RNA replication on co-opted host factors. Nat. Rev. Microbiol. 10 (2), 137–149.
Nagy, P.D., Pogany, J., Lin, J.Y., 2014. How yeast can be used as a genetic platform to explore virus-host interactions: from 'omics' to functional studies. Trends Microbiol. 22 (6), 309–316.
Nagy, P.D., Wang, R.Y., Pogany, J., Hafren, A., Makinen, K., 2011. Emerging picture of host chaperone and cyclophilin roles in RNA virus replication. Virology 411 (2), 374–382.
Neufeldt, C.J., Cortese, M., Acosta, E.G., Bartenschlager, R., 2018. Rewiring cellular networks by members of the Flaviviridae family. Nat. Rev. Microbiol. 16 (3), 125–142.
Panavas, T., Hawkins, C.M., Panaviene, Z., Nagy, P.D., 2005a. The role of the p33:p33/p92 interaction domain in RNA replication and intracellular localization of p33 and p92 proteins of Cucumber necrosis tombusvirus. Virology 338 (1), 81–95.
Panavas, T., Nagy, P.D., 2003. Yeast as a model host to study replication and recombination of defective interfering RNA of Tomato bushy stunt virus. Virology 314 (1), 315–325.
Panavas, T., Serviene, E., Brasher, J., Nagy, P.D., 2005b. Yeast genome-wide screen reveals dissimilar sets of host genes affecting replication of RNA viruses. Proc. Natl. Acad. Sci. U. S. A. 102 (20), 7326–7331.
Panaviene, Z., Baker, J.M., Nagy, P.D., 2003. The overlapping RNA-binding domains of p33 and p92 replicase proteins are essential for tombusvirus replication. Virology 308 (1), 191–205.
Panaviene, Z., Panavas, T., Nagy, P.D., 2005. Role of an internal and two 3'-terminal RNA elements in assembly of tombusvirus replicase. J. Virol. 79 (16), 10608–10618.

Panaviene, Z., Panavas, T., Serva, S., Nagy, P.D., 2004a. Purification of the Cucumber necrosis virus replicase from yeast cells: role of coexpressed viral RNA in stimulation of replicase activity. J. Virol. 78 (15), 8254–8263.
Panaviene, Z., Panavas, T., Serva, S., Nagy, P.D., 2004b. Purification of the cucumber necrosis virus replicase from yeast cells: role of coexpressed viral RNA in stimulation of replicase activity. J. Virol. 78 (15), 8254–8263.
Patury, S., Miyata, Y., Gestwicki, J.E., 2009. Pharmacological targeting of the Hsp70 chaperone. Curr. Top. Med. Chem. 9 (15), 1337–1351.
Pogany, J., Nagy, P.D., 2008. Authentic replication and recombination of Tomato bushy stunt virus RNA in a cell-free extract from yeast. J. Virol. 82 (12), 5967–5980.
Pogany, J., Nagy, P.D., 2012. p33-Independent activation of a truncated p92 RNA-dependent RNA polymerase of tomato bushy stunt virus in yeast cell-free extract. J. Virol. 86 (22), 12025–12038.
Pogany, J., Nagy, P.D., 2015. Activation of tomato bushy stunt virus RNA-dependent RNA polymerase by cellular heat shock protein 70 is enhanced by phospholipids in vitro. J. Virol. 89 (10), 5714–5723.
Pogany, J., Panavas, T., Serviene, E., Nawaz-ul-Rehman, M.S., P, D.N., 2010. A high-throughput approach for studying virus replication in yeast. *Curr Protoc Microbiol* **Chapter** 16. Unit16J.1.
Pogany, J., Stork, J., Li, Z., Nagy, P.D., 2008. In vitro assembly of the Tomato bushy stunt virus replicase requires the host Heat shock protein 70. Proc. Natl. Acad. Sci. U. S. A. 105 (50), 19956–19961.
Pogany, J., White, K.A., Nagy, P.D., 2005. Specific binding of tombusvirus replication protein p33 to an internal replication element in the viral RNA is essential for replication. J. Virol. 79 (8), 4859–4869.
Pratt, W.B., Gestwicki, J.E., Osawa, Y., Lieberman, A.P., 2014. Targeting hsp90/hsp70-based protein quality control for treatment of adult onset neurodegenerative diseases. Annu. Rev. Pharmacol. Toxicol.
Rosenzweig, R., Nillegoda, N.B., Mayer, M.P., Bukau, B., 2019. The Hsp70 chaperone network. Nat. Rev. Mol. Cell Biol. 20 (11), 665–680.
Rousaki, A., Miyata, Y., Jinwal, U.K., Dickey, C.A., Gestwicki, J.E., Zuiderweg, E.R., 2011. Allosteric drugs: the interaction of antitumor compound MKT-077 with human Hsp70 chaperones. J. Mol. Biol. 411 (3), 614–632.
Sanfacon, H., 2017. Grand challenge in plant virology: understanding the impact of plant viruses in model plants, in agricultural crops, and in complex ecosystems. Front. Microbiol. 8, 860.
Sasvari, Z., Izotova, L., Kinzy, T.G., Nagy, P.D., 2011. Synergistic roles of eukaryotic translation elongation factors 1Bgamma and 1A in stimulation of tombusvirus minus-strand synthesis. PLoS Pathog. 7 (12), e1002438.
Sasvari, Z., Lin, W., Inaba, J.I., Xu, K., Kovalev, N., Nagy, P.D., 2020. Co-opted cellular Sac1 lipid phosphatase and PI(4)P phosphoinositide are key host factors during the biogenesis of the tombusvirus replication compartment. J. Virol. 94 (12).
Serva, S., Nagy, P.D., 2006. Proteomics analysis of the tombusvirus replicase: hsp70 molecular chaperone is associated with the replicase and enhances viral RNA replication. J. Virol. 80 (5), 2162–2169.
Serviene, E., Shapka, N., Cheng, C.P., Panavas, T., Phuangrat, B., Baker, J., Nagy, P.D., 2005. Genome-wide screen identifies host genes affecting viral RNA recombination. Proc. Natl. Acad. Sci. U. S. A. 102 (30), 10545–10550.
Shah Nawaz-Ul-Rehman, M., Reddisiva Prasanth, K., Baker, J., Nagy, P.D., 2013. Yeast screens for host factors in positive-strand RNA virus replication based on a library of temperature-sensitive mutants. Methods 59 (2), 207–216.
Sharma, M., Sasvari, Z., Nagy, P.D., 2010. Inhibition of sterol biosynthesis reduces tombusvirus replication in yeast and plants. J. Virol. 84 (5), 2270–2281.
Sharma, M., Sasvari, Z., Nagy, P.D., 2011. Inhibition of phospholipid biosynthesis decreases the activity of the tombusvirus replicase and alters the subcellular localization of replication proteins. Virology 415 (2), 141–152.
Shulla, A., Randall, G., 2012. Hepatitis C virus-host interactions, replication, and viral assembly. Curr Opin Virol 2 (6), 725–732.
Stork, J., Kovalev, N., Sasvari, Z., Nagy, P.D., 2011. RNA chaperone activity of the tombusviral p33 replication protein facilitates initiation of RNA synthesis by the viral RdRp in vitro. Virology 409 (2), 338–347.
Sung, D.Y., Vierling, E., Guy, C.L., 2001. Comprehensive expression profile analysis of the Arabidopsis Hsp70 gene family. Plant Physiol. 126 (2), 789–800.
Taguwa, S., Maringer, K., Li, X., Bernal-Rubio, D., Rauch, J.N., Gestwicki, J.E., Andino, R., Fernandez-Sesma, A., Frydman, J., 2015. Defining Hsp70 subnetworks in dengue virus replication reveals key vulnerability in flavivirus infection. Cell 163 (5), 1108–1123.
Taguwa, S., Yeh, M.T., Rainbolt, T.K., Nayak, A., Shao, H., Gestwicki, J.E., Andino, R., Frydman, J., 2019. Zika virus dependence on host Hsp70 provides a protective strategy against infection and disease. Cell Rep. 26 (4), 906–920 e3.
Verchot, J., 2012. Cellular chaperones and folding enzymes are vital contributors to membrane bound replication and movement complexes during plant RNA virus infection. Front. Plant Sci. 3, 275.
Wang, A., 2015. Dissecting the molecular network of virus-plant interactions: the complex roles of host factors. Annu. Rev. Phytopathol. 53, 45–66.
Wang, A.M., Miyata, Y., Klinedinst, S., Peng, H.M., Chua, J.P., Komiyama, T., Li, X., Morishima, Y., Merry, D.E., Pratt, W.B., Osawa, Y., Collins, C.A., Gestwicki, J.E., Lieberman, A.P., 2013. Activation of Hsp70 reduces neurotoxicity by promoting polyglutamine protein degradation. Nat. Chem. Biol. 9 (2), 112–118.
Wang, R.Y., Stork, J., Nagy, P.D., 2009a. A key role for heat shock protein 70 in the localization and insertion of tombusvirus replication proteins to intracellular membranes. J. Virol. 83 (7), 3276–3287.
Wang, R.Y., Stork, J., Pogany, J., Nagy, P.D., 2009b. A temperature sensitive mutant of heat shock protein 70 reveals an essential role during the early steps of tombusvirus replication. Virology 394 (1), 28–38.
Wang, W., Vinocur, B., Shoseyov, O., Altman, A., 2004. Role of plant heat-shock proteins and molecular chaperones in the abiotic stress response. Trends Plant Sci. 9 (5), 244–252.
Wang, X., Cao, X., Liu, M., Zhang, R., Zhang, X., Gao, Z., Zhao, X., Xu, K., Li, D., Zhang, Y., 2018. Hsc70-2 is required for Beet black scorch virus infection through interaction with replication and capsid proteins. Sci. Rep. 8 (1), 4526.
Weber-Lotfi, F., Dietrich, A., Russo, M., Rubino, L., 2002. Mitochondrial targeting and membrane anchoring of a viral replicase in plant and yeast cells. J. Virol. 76 (20), 10485–10496.
Xu, K., Huang, T.S., Nagy, P.D., 2012. Authentic in vitro replication of two tombusviruses in isolated mitochondrial and endoplasmic reticulum membranes. J. Virol. 86 (23), 12779–12794.
Xu, K., Lin, J.Y., Nagy, P.D., 2014. The hop-like stress-induced protein 1 cochaperone is a novel cell-intrinsic restriction factor for mitochondrial tombusvirus replication. J. Virol. 88 (16), 9361–9378.
Xu, K., Nagy, P.D., 2015a. RNA virus replication depends on enrichment of phosphatidylethanolamine at replication sites in subcellular membranes. Proc. Natl. Acad. Sci. U. S. A. 112 (14), E1782–E1791.
Yasunaga, A., Hanna, S.L., Li, J., Cho, H., Rose, P.P., Spiridigliozzi, A., Gold, B., Diamond, M.S., Cherry, S., 2014. Genome-wide RNAi screen identifies broadly-acting host factors that inhibit arbovirus infection. PLoS Pathog. 10 (2), e1003914.
Zhang, Z., He, G., Filipowicz, N.A., Randall, G., Belov, G.A., Kopek, B.G., Wang, X., 2019. Host lipids in positive-strand RNA virus genome replication. Front. Microbiol. 10, 286.
Zuiderweg, E.R., Bertelsen, E.B., Rousaki, A., Mayer, M.P., Gestwicki, J.E., Ahmad, A., 2013. Allostery in the Hsp70 chaperone proteins. Top. Curr. Chem. 328, 99–153.
Zuiderweg, E.R., Hightower, L.E., Gestwicki, J.E., 2017. The remarkable multivalency of the Hsp70 chaperones. Cell Stress Chaperones 22 (2), 173–189.